Current Research in Toxicology 3 (2022) 100087

Contents lists available at ScienceDirect

Current Research in Toxicology

journal homepage: www.journals.elsevier.com/current-research-in-toxicology

Interaction between mono-(2-ethylhexyl) phthalate and retinoic acid alters Sertoli cell development during fetal mouse testis cord morphogenesis

Maha A. Alhasnani (الحسناني مها)[a,1], Skylar Loeb[a,1], Susan J. Hall[a], Zachary Caruolo[a], Faith Simmonds[a], Amanda E. Solano[a], Daniel J. Spade[a,*]

[a] Department of Pathology and Laboratory Medicine, Brown University, Box G-E5, Providence, RI 02912, USA

ARTICLE INFO

Keywords:
Retinoic acid
Sertoli cell
Fetal testis development
Phthalate toxicity

ABSTRACT

Phthalic acid esters (phthalates) are a class of industrial chemicals that cause developmental and reproductive toxicity, but there are significant gaps in knowledge of phthalate toxicity mechanisms. There is evidence that phthalates disrupt retinoic acid signaling in the fetal testis, potentially disrupting control of spatial and temporal patterns of testis development. Our goal was to determine how a phthalate would interact with retinoic acid signaling during fetal mouse testis development. We hypothesized that mono-(2-ethylhexyl) phthalate (MEHP) would exacerbate the adverse effect of all-trans retinoic acid (ATRA) on seminiferous cord development in the mouse fetal testis. To test this hypothesis, gestational day (GD) 14 C57BL/6 mouse testes were isolated and cultured on media containing MEHP, ATRA, or a combination of both compounds. Cultured testes were collected for global transcriptome analysis after one day in culture and for histology and immunofluorescent analysis of Sertoli cell differentiation after three days in culture. ATRA disrupted seminiferous cord morphogenesis and induced aberrant FOXL2 expression. MEHP alone had no significant effect on cord development, but combined exposure to MEHP and ATRA increased the number of FOXL2-positive cells, reduced seminiferous cord number, and increased testosterone levels, beyond the effect of ATRA alone. In RNA-seq analysis, ATRA treatment and MEHP treatment resulted in differential expression of genes 510 and 134 genes, respectively, including 70 common differentially expressed genes (DEGs) between the two treatments, including genes with known roles in fetal testis development. MEHP DEGs included RAR target genes, genes involved in angiogenesis, and developmental patterning genes, including members of the homeobox superfamily. These results support the hypothesis that MEHP modulates retinoic acid signaling in the mouse fetal testis and provide insight into potential mechanisms by which phthalates disrupt seminiferous cord morphogenesis.

Introduction

Fetal testis development involves coordination of supporting cell differentiation, endothelial cell migration, assembly of Sertoli cells and germ cells to form cords, and secretion of basement membrane components by Sertoli and peritubular myoid cells. Exposure to phthalic acid esters (phthalates) can disrupt testis development and has been linked to later life reproductive disorders (Manikkam et al., 2012, Manikkam et al., 2013). Phthalates are high-production volume compounds used to impart plasticity to polyvinyl chloride (PVC) products, including some plastic containers, medical devices, and food packaging, and are also used in the formulation of personal care products, industrial lubricants, and adhesives (Benjamin et al., 2015). Phthalates are not covalently bound to the PVC polymer and therefore can leach into the surrounding environment, resulting in human exposure. The most common route of exposure to phthalates is ingestion, after which the intestine and liver metabolize phthalate diesters into their toxic phthalate monoester metabolites (Albro, 1986, Kavlock et al., 2006, Kavlock et al., 2002). In

Abbreviations: ATRA, All-trans retinoic acid. CAS # 302-79-4; DMSO, dimethyl sulfoxide; GD, gestational day; GO, Gene Ontology; IPA, Ingenuity Pathway Analysis; ITCN, Image-based Tool for Counting Nuclei; MEHP, mono-(2-ethylheyxl) phthalate. CAS # 4376-20-9; MNGs, multinucleated germ cells; PVC, polyvinyl chloride; TDS, testicular dysgenesis syndrome.

* Corresponding author at: Department of Pathology and Laboratory Medicine, Brown University, Providence, RI 02912, USA.
E-mail addresses: maha_alhasnani@brown.edu (M.A. Alhasnani), skylar_loeb@alumni.brown.edu (S. Loeb), susan_hall@brown.edu (S.J. Hall), faith_simmonds@brown.edu (F. Simmonds), asolano02.student@mountsaintvincent.edu (A.E. Solano), daniel_spade@brown.edu (D.J. Spade).

[1] Authors contributed equally to the manuscript.

https://doi.org/10.1016/j.crtox.2022.100087
Received 14 March 2022; Received in revised form 17 September 2022; Accepted 17 September 2022
Available online 21 September 2022

pregnant women, phthalate monoesters can cross the placenta and induce harmful effects upon the fetus, which is the most vulnerable life stage for phthalate-induced testicular toxicity (Kavlock et al., 2006, Kavlock et al., 2002, Wang et al., 2016).

Phthalate-induced fetal male reproductive toxicity is species-dependent (Johnson et al., 2012). In the rat, phthalates significantly reduce testosterone production (Spade et al., 2018, Hannas et al., 2011b, Gray et al., 2000, Parks et al., 2000, Mylchreest et al., 2002). In addition to reduced testosterone, phthalate exposure in fetal rats results in a phenotype that resembles the testicular dysgenesis syndrome (TDS), including male reproductive tract malformations such as hypospadias and cryptorchidism and the induction of multinucleated germ cells (MNGs) in the fetal testis (Foster, 2006, Spade et al., 2015, Ferrara et al., 2006). In the fetal mouse, there have been multiple reports that phthalates do not reduce testosterone synthesis. However, phthalate exposure in the fetal mouse causes germ cell apoptosis, the induction of MNGs, impaired development of Sertoli cells, alterations in the diameter and morphology of seminiferous cords, and changes in the expression of genes that code for steroid biosynthesis proteins (Gaido et al., 2007, Heger et al., 2012, van den Driesche et al., 2012, Johnson et al., 2012, Wang et al., 2016, Johnson et al., 2011), indicating that mechanisms in addition to impaired testosterone synthesis contribute to phthalate toxicity in the fetal testis.

Several signaling processes that are required for normal testis development are plausible targets of phthalates. Phthalates are peroxisome proliferators. However, PPARα is unnecessary for some toxic effects of phthalates, and phthalates do not induce a typical PPAR-mediated gene expression response in the fetal testis (Bhattacharya et al., 2005, Hannas et al., 2012, Gray et al., 2021). Another possible target is retinoic acid (RA) signaling. All-trans retinoic acid (ATRA) is the active metabolite of Vitamin A (retinol) and the natural ligand of retinoic acid receptors (RARs), which act by forming heterodimers with retinoid X receptors (RXRs) to induce or repress expression of downstream genes, many of which promote cell differentiation during organogenesis and developmental patterning (Cunningham and Duester, 2015). ATRA is also a potent driver of gonocyte differentiation. After gonadal sex determination, supporting cells differentiate into Sertoli cells, which express the retinoic acid-degrading cytochrome P450 enzyme, CYP26B1. In the fetal testis, *Sox9* up-regulates the expression of *Cyp26b1* to prevent ATRA entry into the testis, while in the fetal ovary, *Foxl2* down-regulates the expression of *Cyp26b1* to allow ATRA to enter the gonad and drive germ cell entry into meiosis (Kashimada et al., 2011, Nicol et al., 2018). Disruption of the fetal testicular retinoic acid concentration by introducing exogenous retinoic acid can impair cord formation and induce germ cell death (Livera et al., 2000, Spade et al., 2019a, Trautmann et al., 2008, Bowles et al., 2018, Lambrot et al., 2006).

Multiple studies have shown that phthalates interact with the RA signaling pathway in the fetal testis. In one study, mono-(2-ethylheyxl) phthalate (MEHP) and ATRA competition for RXRs prevented RARα translocation to the mouse Sertoli cell nucleus (Dufour et al., 2003). Another study found that MEHP significantly inhibited RA signaling during both short- and long-term exposure periods using an in vitro screen (Chen and Reese, 2016). In a previous study using a rat fetal testis culture model, we reported that MEHP enhanced the effect of ATRA on expression of genes related to sex determination but opposed seminiferous cord loss caused by ATRA (Spade et al., 2019b). This study provided evidence of an interaction between MEHP and ATRA in the fetal rat testis but left several mechanistic questions unanswered. In particular, because the mouse fetal testis is resistant to the anti-androgenic effect of phthalates, similar to the human fetal testis (Johnson et al., 2012), the mouse model would allow us to test how this interaction affects seminiferous cord development in the absence of altered testosterone levels. Here, we aimed to determine how MEHP and ATRA would affect testicular spatial patterning and the development of supporting cells in *ex vivo* cultured fetal mouse testes. We hypothesized that MEHP would exacerbate the adverse effect of ATRA on seminiferous cord development in the mouse fetal testis. To test this hypothesis, mouse fetal testes were cultured for 1–3 days with ATRA, MEHP, or a combination of both compounds, and were analyzed for morphological alterations and changes in gene expression involved in supporting cell differentiation and structural development of the seminiferous cords. In the mouse, seminiferous cord formation begins on GD 11–12, as described in a review by Brennan and Capel (2004). We chose to use a GD 14 *ex vivo* culture system in this study to characterize the effect of phthalates on testis morphogenesis starting at a point after initial seminiferous cord development. This allowed us to compare effects of ATRA and MEHP across species with our prior publications on rat fetal testis, and to compare with mouse *in vivo* phthalate toxicity studies from the literature.

Materials and methods

Animals

All procedures that involved the use of animals were approved by the Brown University Institutional Animal Care and Use Committee and are consistent with the Guide for the Care and Use of Laboratory Animals. Timed pregnant C57BL/6 mice (strain code 027) were procured from Charles River Laboratories (Wilmington, Massachusetts). On gestational day (GD) 14, dams were euthanized by inhalation of 5 % isoflurane. Fetuses were euthanized by decapitation and dissected under a stereomicroscope. Fetal gonads were examined to determine the sex of the fetus, and fetal testes were isolated for *ex vivo* culture. Testes were cleanly dissected from mesonephroi to eliminate mesonephric retinoic acid contribution to the culture.

Fetal testis culture

When working with ATRA, all plates and solutions were handled under yellow light. Stock solutions of 0.1 M ATRA and 0.67 M MEHP were prepared in dimethyl sulfoxide (DMSO) vehicle. Stock solutions were aliquoted in amber glass vials to avoid exposure to fluorescent light and stored at −20 °C for no more than 14 days after preparation. Testes were cultured on Millicell-CM cell culture inserts (EMD-Millipore, Billerica, Massachusetts) in Falcon 24-well cell culture plates (Corning Life Sciences, Tewksbury, Massachusetts) with 480 μL Dulbecco's Modified Eagle Medium/Nutrient Mixture F12 (Gibco/Thermo Fisher Scientific, Waltham, Massachusetts) containing 20 μg/mL gentamicin (Gibco), 50 units/mL penicillin (Gibco), 50 μg/mL streptomycin (Gibco), 50 μg/mL Albumax II (Gibco), 200 μg/mL bovine serum albumin (Sigma Aldrich, St. Louis, Missouri), 1X ITS liquid medium supplement (Sigma Aldrich), and 50 μg/mL sodium L-ascorbate (Sigma Aldrich). Treatment compounds were added directly to culture media as follows. For each testis pair isolated from a single fetus, one testis was cultured in vehicle control media (1:4000 DMSO in culture media), while the contralateral testis was cultured in media containing 10^{-8}, 10^{-7}, or 10^{-6} M ATRA, 10^{-6}, 10^{-5}, or 10^{-4} M MEHP, or a combination of 10^{-6} M ATRA with 10^{-6}, 10^{-5}, or 10^{-4} M MEHP (referred to as "co-exposure"). After 1 day of culture, testes were collected for RNA extraction and gene expression analysis. This early time point was chosen so that RNA-seq analysis would identify gene expression changes resulting from immediate activation of nuclear receptor signaling, but not changes that result from altered tissue structure or proportional changes in various testicular cell populations after multiple days in culture. After 3 days of culture, the remaining samples were fixed in modified Davidson's solution for 15 min, and then stored in 70 % ethanol at 4 °C until processing for histology and immunofluorescence analyses. After 3 days of culture, day 3 (48–72 h) media was snap-frozen and stored at −80 °C for testosterone analysis.

Histology

Fixed samples were dehydrated in a series of graded ethanols, followed by three changes of xylene, and embedded in paraffin as described in our previous publications (Spade et al., 2019a, Spade et al., 2019b). Briefly, paraffin-embedded samples were cut from paraffin blocks, oriented perpendicular to the block face, and re-embedded to allow consistent transverse sections. Paraffin sections were cut at a thickness of 5 μm and mounted onto glass slides. To obtain representative histological data, paraffin sections were obtained for hematoxylin and eosin (H&E) staining at depths of 150, 300, 450, and 600 μm. Additional sections were retained for immunofluorescence analysis between the 150 and 450 μm cutting depths. For histological analysis, sections were deparaffinized in three changes of xylene, rehydrated in graded ethanols, and stained with H&E. H&E sections were visualized using an Olympus BH-2 light microscope at 100–200X total magnification, and the number of intact seminiferous cords and number of multinucleated germ cells per section was manually counted. Sections from each group were selected at random and scanned with an Aperio ScanScope CS at 40X magnification for presentation in figures.

Immunofluorescence

Immunofluorescent labeling was performed for the germ cell marker, germ cell nuclear antigen (GCNA/TRA98), the Sertoli cell marker, SRY-box transcription factor 9 (SOX9), and the granulosa cell-associated transcription factor, forkhead box L2 (FOXL2), using paraffin sections of cultured testes. Adult mouse ovary and testis sections obtained from other experiments were used as positive controls for FOXL2 and SOX9, respectively. Tissue sections were deparaffinized in xylenes and rehydrated through a series of graded ethanols. Antigen retrieval was performed by heating the sections in 10 mM citrate buffer, pH 6.0, in a vegetable steamer for 20 min, and then cooling at room temperature for an additional 20 min. Sections were permeabilized in 0.1 % sodium citrate with 0.1 % Triton X-100 for 5 min. For sections on which FOXL2 labeling was performed, sections were incubated in 3 % hydrogen peroxide diluted in methanol for 60 min to block endogenous peroxidase activity and an Avidin/Biotin Blocking Kit (Vector Laboratories, Burlingame, CA) was used to block endogenous avidin and biotin. All sections were incubated for 20 min in a blocking buffer consisting of 8 % normal donkey serum and 1 % bovine serum albumin in PBS. Sections were incubated with primary antibodies diluted in blocking buffer overnight at 4 °C in a humidified chamber. A no-primary antibody negative control was run for each sample. Sections were incubated with secondary antibody diluted in blocking buffer for 60 min at room temperature. Antibodies and dilutions are described in Table 1. For GCNA and SOX9, a fluorophore-conjugated secondary antibody was used. For FOXL2, the sections were incubated with Vector Laboratories VECTASTAIN Elite ABC Kit following application of the secondary antibody, and signal was developed using the Alexa Fluor 488 Tyramide SuperBoost Kit (Thermo Fisher Scientific). All samples were counterstained with Hoechst 33342 (Thermo Fisher Scientific), and coverslips were mounted with Prolong Gold Mounting Media (Thermo Fisher Scientific). The samples from the MEHP, ATRA and co-exposure experiments were imaged using a Zeiss Axiovert 200 M, Axiovert A1 (ZEISS Microscopy, Jena, Germany), or Olympus VS200 (Olympus, Tokyo, Japan) fluorescence Microscope to be used for cell counting. The total SOX9-positive cell count, FOXL2-positive cell count, and Hoechst-positive cell count were obtained for each sample. Cell counts were performed on raw tiff images, using the Image-based Tool for Counting Nuclei (ITCN) plugin in ImageJ. FOXL2 and SOX9 positivity rate were calculated using Hoescht-positive cells as the denominator. For example, % SOX9-positive cells were calculated for each section as the ratio of total SOX9-positive cells to total Hoescht-positive cells, multiplied by 100. The ITCN plugin was also used to analyze Sertoli cell localization by counting the proportion of total SOX9-positive cells that were located in intact seminiferous cords. GCNA-positive cell counts in the co-exposure experiment were obtained in the same manner as the SOX9 and FOXL2 counts. For GCNA-labeled germ cells in sections from the ATRA and MEHP dose–response experiments, germ cells were counted by scoring the original image files (.vsi) from the Olympus VS200 slide scanner in QuPath.

RNA sequencing

RNA-seq analysis was performed on testes cultured for 1 day in 10^{-4} M MEHP, 10^{-6} M ATRA, and 10^{-4} M MEHP + 10^{-6} M ATRA and contralateral vehicle-treated testes as a common control group. Snap-frozen fetal testes were homogenized in Trizol (ThermoFisher Scientific) using zirconium oxide beads in a NextAdvance Bullet Blender Storm 24 and extracted using chloroform, per the manufacturer's instructions. RNA was purified from the aqueous phase of the Trizol extraction using the Arcturus PicoPure kit (ThermoFisher Scientific) according to the manufacturer's protocol, including the optional on-column DNase digestion. The concentration and purity of RNA were assessed using a NanoDrop ND-1000 spectrophotometer (ThermoFisher) and Qubit 2.0 Fluorometer, and the integrity of RNA was determined using a TapeStation System (Agilent Technologies, Palo Alto, CA, USA). RNA samples used for RNA-seq analysis had A_{260}/A_{280} values ranging from 1.72 to 2.01, with a mean of 1.85. The average RIN was 9.72 and the average DV200 was 90.88 with a minimum value of 9.4 and 88.43 for RIN and DV200, respectively. RNA Libraries were prepared and sequenced by Genewiz (NJ, US). Libraries were constructed from a minimum of 488.9 ng RNA using the NEBNext Ultra II RNA library prep kits for Illumina with the polyA selection method using manufacturer's instructions (New England Biolabs, Ipswich, MA, USA) and sequenced on an Illumina HiSeq 4000 system in 2x150bp paired-end configuration.

Testosterone analysis

Media samples from the third day of culture with 10^{-6} M ATRA, 10^{-4} M MEHP, 10^{-6} M ATRA + 10^{-4} M MEHP, and contralateral vehicle samples were sent to the Ligand Assay and Analysis Core at the University of Virginia for testosterone analysis. Testosterone secreted into the media was measured using a mouse and rat testosterone ELISA (Immuno-Biological Laboratories, Inc., Minneapolis, MN). The reported intra- and inter-assay coefficients of variation for all samples tested by this method in 2020 were 6.0 % and 9.3 %, respectively. Samples were

Table 1
Antibodies used for Immunofluorescence.

Antibody Type	Species	Target	Conjugate	Manufacturer	Product No.	Dilution
Primary	Rabbit	SOX9	none	Millipore Sigma	ab5535	1:500
Primary	Goat	FOXL2	none	Abcam	ab5096	1:4000
Primary	Rat	GCNA	none	Abcam	ab82527	1:500
Secondary	Donkey	Rabbit IgG	Alexa Fluor 568	Thermo Fisher	A10042	1:2000
Secondary	Donkey	Goat IgG	biotin	Millipore	AP180b	1:400
Secondary	Goat	Rat IgG	Alexa Fluor 488	Thermo Fisher	A11006	1:200
Secondary	Goat	Rabbit IgG	Alexa Fluor 488	Thermo Fisher	A32731	1:200
Secondary	Goat	Rat IgG	Alexa Fluor 568	Thermo Fisher	A11077	1:200

diluted 1:10 to achieve a concentration within the reportable range of 10–1600 ng/dl and tested in duplicate.

Data analysis and statistics

Histology, immunofluorescence, and testosterone data were summarized using Excel and analyzed using GraphPad Prism version 9 (GraphPad Software, San Diego, CA). The sample size for each analysis is stated in the corresponding figure legend. All samples cultured in vehicle media were treated statistically as a single group. The normality of the data from each treatment group was tested using the Shapiro-Wilk test. For concentration–response data, if data were normally distributed, differences between treatment groups were tested using one-way ANOVA, followed by Dunnet's post hoc test for multiple comparisons and a separate post-hoc test for linear trend. If the data were not normally distributed, differences between treatment groups were tested using a Kruskal-Wallis test, followed by Dunn's test for multiple comparisons, relative to the vehicle control. For MEHP and ATRA combined exposure experiments, if the data were normally distributed, differences between groups were tested using one-way ANOVA followed by Tukey's test for multiple comparisons. If the data were not normally distributed, the non-parametric Kruskal-Wallis test, followed by Dunn's multiple comparisons test was used to assess all pairwise differences. Data are reported in figures as mean ± SEM. When Tukey's or Dunn's test was used to make all pairwise comparisons, statistical significance was represented in the figures by letters above each bar in the chart; bars that are not connected by a common letter have significantly different means with $p < 0.05$.

RNA alignment and initial RNA-seq analysis was performed by Genewiz. Reads were trimmed and filtered using Trimmomatic v.0.36, then mapped to the mouse reference genome (Mus musculus GRCm38, ENSEMBL) using the STAR aligner v.2.5.2b. Gene hit counts were generated by featureCounts (Subread package v.1.5.2). Raw and normalized RNA-seq data are available from the NCBI Gene Expression Omnibus database (Series GSE195969). Differentially expressed genes (DEGs) were identified using DESeq2 for three comparisons: ATRA, MEHP, and ATRA + MEHP, versus a common vehicle control group. Genes with adjusted p-value < 0.05 and absolute log2 fold change > 1 (Wald test) were considered to be DEGs (n = 4–6 samples/treatment group and 15 vehicle). Gene Ontology (GO) analysis was performed on the statistically significant set of genes using GeneSCF v.1.1-p2 to perform a Fisher exact test with a filter value of < 0.05. The goa_MusMusculus GO list was used to cluster the set of genes, categorizing them based on the biological processes. To analyze the effect of our

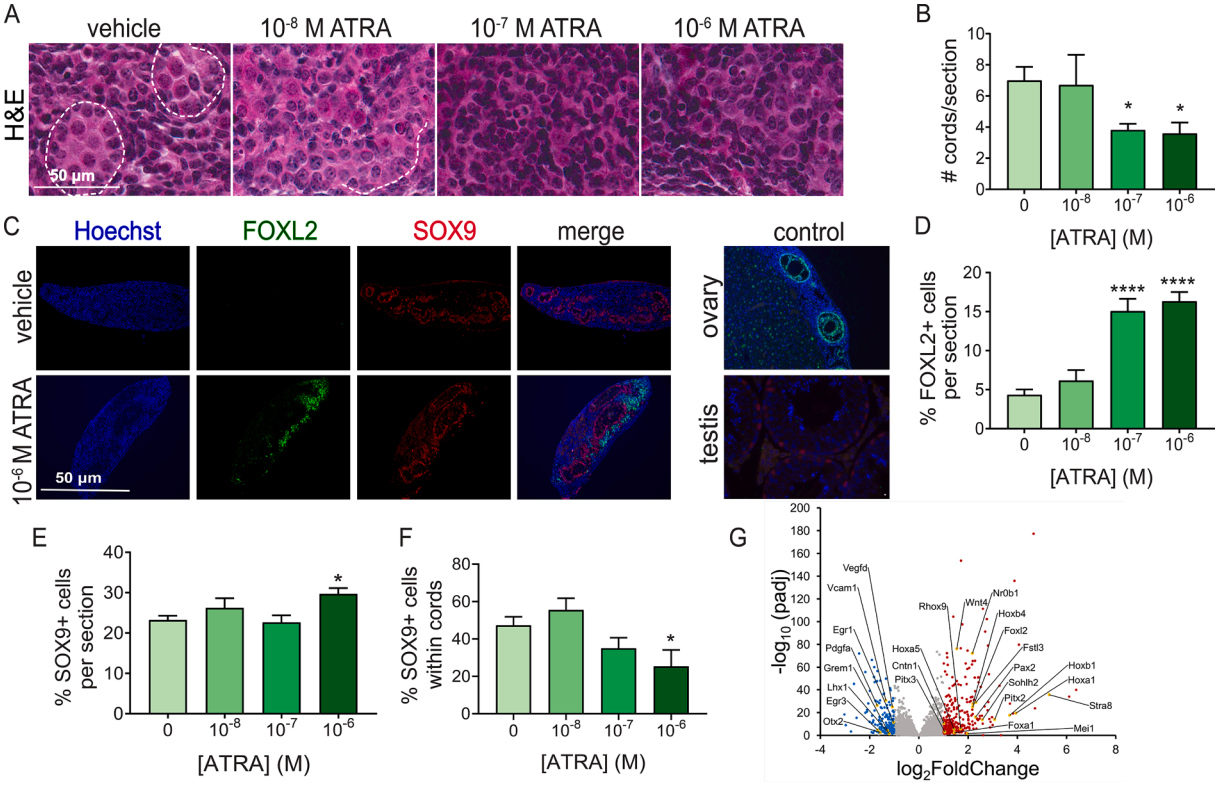

Fig. 1. ATRA diminished seminiferous cord structure and induced FOXL2 expression in fetal mouse testes. A. In H&E-stained tissue sections, following 3 days of culture, vehicle-treated testes contained more intact seminiferous cords than ATRA treated samples. Dashed lines indicate seminiferous cord basement membranes. B. The number of seminiferous cords per histological section was significantly lower in 10^{-7} and 10^{-8} M ATRA treatment samples than vehicle control. *$p < 0.05$ by one-way ANOVA followed by Dunn's test, n = 6–9/group and 20 vehicle. C. FOXL2 expression was induced in testes treated with 10^{-7} M and 10^{-6} M ATRA, and ATRA-treated samples displayed reduced seminiferous cord organization, based on localization of SOX9-positive cells, though this phenotype was variable. FOXL2-positive and SOX9-positive cells were often found in close proximity but were never co-localized. Specificity of the FOXL2 and SOX9 immunofluorescent labeling was confirmed in adult mouse ovary and testis positive control sections, respectively. D. ATRA significantly increased FOXL2-positive cell number in a concentration-dependent fashion ($p < 0.0001$ by test for linear trend), and 10^{-7} and 10^{-6} M ATRA had significantly greater FOXL2-positive cells than vehicle control ****$p < 0.0001$ by ANOVA followed by Dunnet's test. E. SOX9-positive Sertoli cell number was significantly increased in the 10^{-6} M ATRA treatment, relative to control *$p < 0.05$ by Kruskal-Wallis followed by Dunn's test. The % FOXL2-positive cells and % SOX9-positive cells were calculated as the ratio of total cell type marker-positive cells/total Hoescht-positive cells per section, multiplied by 100. F. The percentage of SOX9-positive cells localized to seminiferous cords decreased significantly in a concentration-dependent manner ($p < 0.001$ by test for linear trend) and was significantly lower in the 10^{-6} M ATRA group than vehicle control *$p < 0.05$ by ANOVA followed by Dunnet's test. For all immunofluorescence analyses, n = 6–7/group and 18 vehicle. G. Following 1 day of culture, 10^{-6} M ATRA significantly upregulated 333 genes (red circles), and downregulated 177 genes (blue circles), relative to vehicle control ($q < 0.05$, $|\log2 \text{ fold change}| \geq 2$), n = 5 ATRA and 15 vehicle. Labeled genes are involved in testis development and spatial patterning during development.

treatments on fetal testicular germ cell development, we compared our DEG lists to germ cell stage-specific single cell RNA-seq data (Zhao et al., 2021). We categorized each gene by the developmental stage ("cluster") when it is first expressed, as identified in the single-cell RNA-seq data. We then determined the number of DEGs from each of our RNA-seq analyses (ATRA, MEHP, and MEHP + ATRA vs vehicle) that matched with each single-cell RNA-seq gene cluster.

Results

ATRA adversely affected seminiferous cord development by altering somatic cell identity

We previously found that ATRA antagonized seminiferous cord development in cultured fetal rat testes (Spade et al., 2019a). Here, we tested whether ATRA would have the same effect on the mouse fetal testis and whether we could identify gene expression evidence of the mechanisms by which this happens. Following three days of culture, there was a significant reduction in seminiferous cord number per histological section in testes cultured with 10^{-7} and 10^{-6} M ATRA, relative to the vehicle control (Fig. 1A, 1B). Immunofluorescent analysis revealed the presence of both FOXL2-positive and SOX9-positive cells in most sections, but cells co-expressing both proteins were not observed (Fig. 1C). The percentage of FOXL2-expressing cells was significantly elevated in the 10^{-7} M and 10^{-6} M ATRA treatment groups, and there was a significant positive linear trend with increasing concentrations of ATRA ($p < 0.0001$) (Fig. 1D). The percentage of SOX9-expressing cells was consistent, with a maximum difference of 7 % between groups. However, there was a statistically significant increase in samples treated with 10^{-6} M ATRA, relative to vehicle (Fig. 1E). Although the total number of SOX9-positive cells was consistent, there was a significant negative linear trend between the percent of SOX9-positive cells located within cords and ATRA concentration ($p < 0.01$) (Fig. 1F).

RNA-seq analysis identified 333 upregulated genes and 177 downregulated genes in response to 1 day of culture in ATRA ($q < 0.05$; $|\log2$ fold change$| > 1$) (Fig. 1G, Supplemental Table S1). GO enrichment analysis of the ATRA-treated samples identified 17 significant GO terms (Table 2, Supplemental Table S2), some of which were related to the female reproductive tract development, including oocyte development (GO:0048599) and paramesonephric duct development (GO:0061205); development and spatial patterning of the testis, including anatomical structure formation involved in morphogenesis (GO:0048646), positive regulation of branching involved in ureteric bud morphogenesis (GO:0090190), multicellular organism development (GO:0007275), anterior/posterior pattern specification (GO:0009952), and animal organ morphogenesis (GO:0009887); and retinoic acid metabolism processes, including meiotic cell cycle (GO:0051321), cellular response to retinoic acid (GO:0071300), meiotic telomere clustering (GO:0045141), and retinoic acid catabolic process (GO:0034653).

MEHP altered testicular gene expression without significantly altering seminiferous cord structure

MEHP is known to disrupt spatial patterning in the testis. Here, we sought to test whether exposure to MEHP would antagonize cord development in a manner similar to ATRA. Mouse fetal testes cultured for 3 days in media containing MEHP were mostly histologically normal, with a slight increase in the number of seminiferous cords per section only at the 10^{-5} M concentration (Fig. 2A, 2B). FOXL2-expressing cells were rare, and there was an increasing proportion of FOXL2-positive cells with increasing concentration of MEHP (Fig. 2C). However, there were no significant pairwise differences between the MEHP and vehicle treatment groups, and the highest concentration resulted in only an approximately 3 % increase in FOXL2-expressing cells (Fig. 2D). Immunofluorescent labeling revealed no significant difference in the proportion of SOX9-positive cells between any of the treatment groups (Fig. 2E). MEHP also had no effect on the localization of SOX9-expressing cells across treatment groups (Fig. 2F).

MEHP significantly altered the transcriptome of *ex vivo* 1-day cultured fetal mouse testes. RNA-seq analysis identified 51 upregulated transcripts and 83 downregulated transcripts, relative to vehicle ($p < 0.05$; $|\log2$ fold change$| > 1$) (Fig. 2G, Supplemental Table S3). Enrichment analysis of the MEHP gene expression results identified significantly enriched GO terms related to spatial patterning of the testis, including branching involved in ureteric bud morphogenesis (GO:0001658), anatomical structure formation involved in morphogenesis (GO:0048646), formation of anatomical boundary (GO:0048859), and paramesonephric duct development (GO:0061205) (Table 3, Supplemental Table S4). An analysis was performed in Ingenuity Pathway Analysis (IPA) to identify putative upstream regulators of MEHP-driven gene expression changes. IPA identified all three RAR isoforms, RARα, RARβ, and RAR**γ**, and three PPAR**γ**-selective agonists, pioglitazone, troglitazone and rosiglitazone (Edvardsson et al., 1999), as putative upstream regulators (Fig. 3, Table 4, Supplemental Table S5).

Table 2
Top 17 GO terms obtained by GO term enrichment analysis of ATRA vs vehicle RNA-seq dataset.

GO ID	GO biological process	% DR genes	p-adj
GO:0007275	multicellular organism development	5.20	< 0.001
GO:0009952	anterior/posterior pattern specification	13.4	< 0.001
GO:0007129	synapsis	22.6	0.012
GO:0006937	regulation of muscle contraction	27.3	0.015
GO:0009887	animal organ morphogenesis	10.5	0.021
GO:0050710	negative regulation of cytokine secretion	33.3	0.021
GO:0051965	positive regulation of synapse assembly	12.7	0.021
GO:0051321	meiotic cell cycle	7.50	0.028
GO:0071300	cellular response to retinoic acid	15.9	0.029
GO:0030182	neuron differentiation	9.40	0.029
GO:0021612	facial nerve structural organization	40.0	0.033
GO:0045141	meiotic telomere clustering	40.0	0.033
GO:0034653	retinoic acid catabolic process	75.0	0.041
GO:0048599	oocyte development	33.3	0.041
GO:0048646	anatomical structure formation involved in morphogenesis	22.7	0.041
GO:0061205	paramesonephric duct development	75.0	0.041
GO:0090190	positive regulation of branching involved in ureteric bud morphogenesis	21.7	0.041

Abbreviations: DR = significantly differentially regulated, GO = gene ontology, p-adj = multiplicity adjusted p-value. Summary of significantly enriched GO terms in ATRA versus vehicle control treated samples. The percent of significant DR genes indicates the percent of enriched genes within GO terms, where significance of the enriched term has a q-value of < 0.05. Full results are reported in Supplemental Table S2.

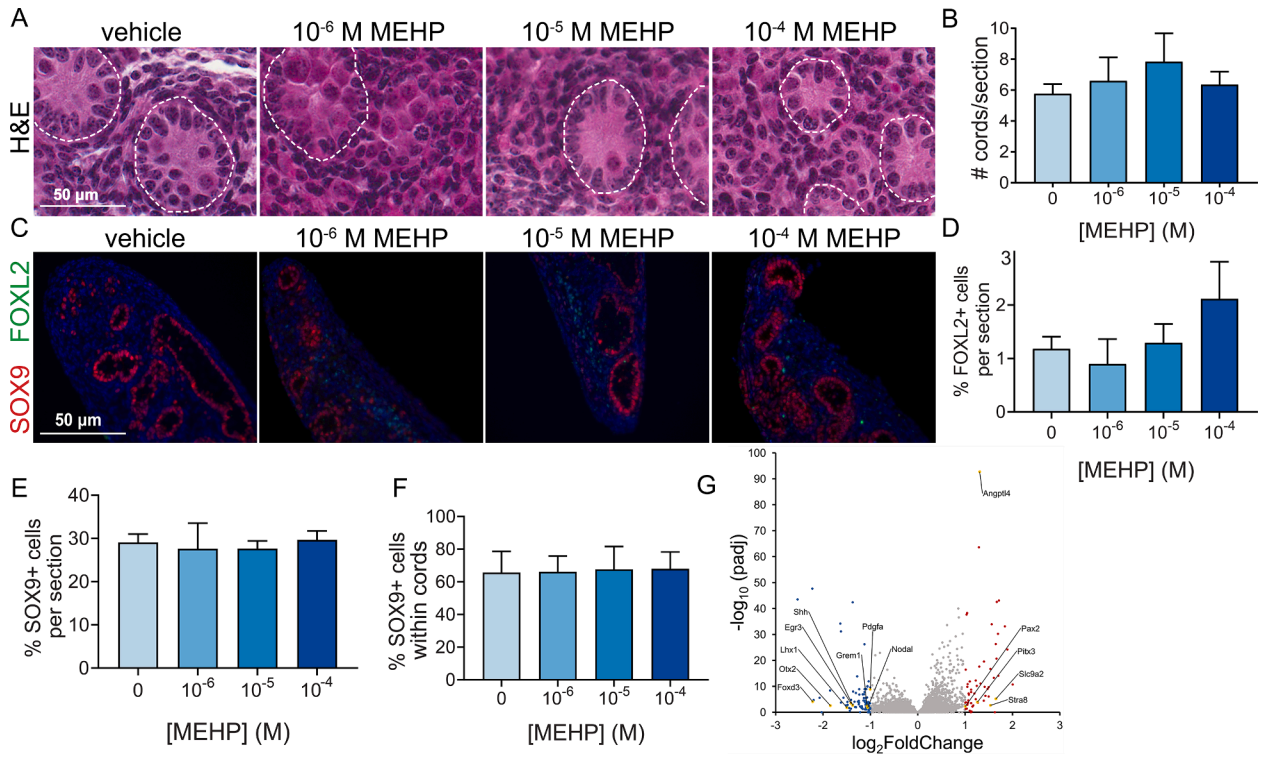

Fig. 2. MEHP significantly altered mouse fetal testis transcriptome but not seminiferous cord morphology. A. MEHP-treated testes showed seminiferous cord organization comparable to vehicle control. Dashed lines indicate seminiferous cord basement membranes. B. The number of seminiferous cords in H&E-stained sections of 3-day MEHP treated samples was not significantly different from vehicle control by one-way ANOVA followed by Dunnet's test, n = 6–7/group and 20 vehicle. C. FOXL2- and SOX9-positive cells were present in all treatment groups. D. MEHP did not significantly induce FOXL2 expression in fetal mouse testicular somatic cells by Kruskal-Wallis followed by Dunn's test. E. SOX9-positive Sertoli cell number varied slightly, with no significant changes in SOX9-positive cell numbers by one-way ANOVA followed by Dunnet's test. F. MEHP had no significant influence on Sertoli cell localization by Kruskal-Wallis followed by Dunn's test. For all immunofluorescence analyses, n = 6–7/group and 20 vehicle. G. Following 1 day in culture, 10^{-4} M MEHP significantly upregulated 51 genes (red circles) and downregulated 83 genes (blue circles), relative to vehicle control ($q < 0.05$, |log2 fold change| >2), n = 6 MEHP and 15 vehicle. Labeled genes are involved in early testis development and spatial patterning.

MEHP enhanced ATRA toxicity in the fetal mouse testis

It has previously been demonstrated that MEHP interacts with retinoic acid signaling in rat fetal testes and cultured mouse Sertoli cells (Spade et al., 2019b, Dufour et al., 2003). Here, we tested whether MEHP would antagonize the effects of ATRA on cultured fetal mouse testes. Exposure of cultured fetal mouse testes to a mixture of ATRA and MEHP for 3 days led to altered testis morphology (Fig. 4). Cord number was significantly lower in samples treated with 10^{-6} M ATRA + 10^{-6} M MEHP, compared to the control (Fig. 4C). In immunofluorescent analysis, there was a significant increase in the percentage of FOXL2-positive cells in samples treated with 10^{-6} M ATRA and 10^{-5} M MEHP combined, with approximately 19 % of cells expressing FOXL2 ($p > 0.031$) (Fig. 4D). There was no significant difference in the percentage of SOX9-positive cells (Fig. 4E) or the localization of SOX9-expressing cells between any of the treatment groups (Fig. 4F). Combined exposure to

Table 3
Top 15 GO terms obtained by GO term enrichment analysis of MEHP vs vehicle RNA-seq dataset.

GO ID	GO biological process	% DR genes	p-adj
GO:0006814	sodium ion transport	5.60	0.014
GO:0071542	dopaminergic neuron differentiation	13.8	0.018
GO:0090009	primitive streak formation	30.0	0.018
GO:0019882	antigen processing and presentation	11.1	0.021
GO:0019886	antigen processing and presentation of exogenous peptide antigen via MHC class II	21.4	0.021
GO:0045060	negative thymic T cell selection	21.4	0.021
GO:0001658	branching involved in ureteric bud morphogenesis	8.70	0.031
GO:0048646	anatomical structure formation involved in morphogenesis	13.6	0.045
GO:0048859	formation of anatomical boundary	50.0	0.045
GO:0061205	paramesonephric duct development	50.0	0.045
GO:0090190	positive regulation of branching involved in ureteric bud morphogenesis	13.0	0.045
GO:0001822	kidney development	4.40	0.047
GO:0002504	antigen processing and presentation of peptide or polysaccharide antigen via MHC class II	40.0	0.047
GO:0006885	regulation of pH	12.0	0.047
GO:0021871	forebrain regionalization	40.0	0.047

Abbreviations: DR = significantly differentially regulated, GO = gene ontology, p-adj = multiplicity adjusted p-value. Summary of significantly enriched GO terms in MEHP versus vehicle control. The percent of significant genes indicates the percent of enriched gene within GO terms, where significance of the enriched term has a q-value of < 0.04. Full results are reported in Supplemental Table S4.

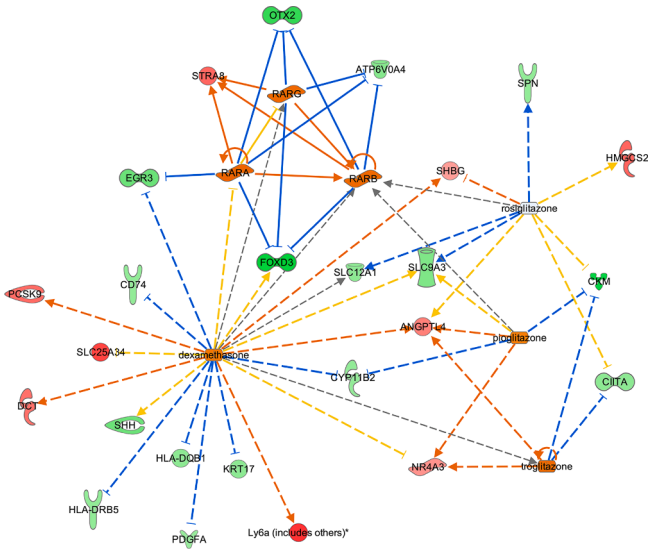

Fig. 3. MEHP gene expression suggests regulation by multiple nuclear receptors. Pathway diagram showing connections between significantly differentially regulated genes in the MEHP vs vehicle RNA-seq analysis, following one day of culture with vehicle control or 10^{-4} M MEHP, as described in Fig. 2, that are connected to putative upstream regulators predicted by Ingenuity Pathway Analysis (Table 4). Predicted upstream regulators included RARα, RARβ, RARγ, dexamethasone, troglitazone, pioglitazone, and rosiglitazone. Red: upregulated; green: downregulated. Arrows show direction of regulation (solid: direct regulation; dashed line: indirect regulation). Blunt arrows show inhibition.

ATRA and MEHP resulted in a slight depletion in germ cell count compared to vehicle, but this was not statistically significant (Fig. 4G).

RNA-seq analysis of samples cultured with 10^{-4} M MEHP and 10^{-6} M ATRA for 1 day detected a total of 1102 significant DEGs, including 495 genes that were upregulated, and 608 genes downregulated relative to vehicle control ($p < 0.05$; $|\log2 \text{ fold change}| > 1$) (Fig. 4H, Supplemental Table S6). Significantly enriched GO terms in the co-exposure study were related to spatial patterning of the testis, including multicellular organism development (GO:0007275) and anterior/posterior pattern specification (GO:0009952) (Table 5, Supplemental Table S7). Of the 1102 differentially regulated transcripts in the co-exposure, 453 and 119 were also differentially regulated by ATRA and MEHP, respectively. 69 genes were differentially regulated by all three treatments, relative to vehicle. Only *Cyp11b1* was regulated in opposite directions by ATRA and MEHP and not differentially regulated in the co-exposure (Fig. 5). Among the 69 genes that were differentially regulated in all three comparisons were several genes critical for early testis development and spatial patterning. Also included were genes, such as *Ciita* and *H2-ab1*, that are involved in macrophage function, which has been recognized as a critical component of early testis patterning (DeFalco et al., 2014) (Fig. 5). Consistent with the ATRA and MEHP treatments causing differential regulation of many of the same genes, 51 characterized RAR target genes (Balmer and Blomhoff, 2002) were differentially regulated by at least one treatment, including 9 that were differentially regulated by MEHP (Fig. 5A, 5B, Supplemental Table S8). The ATRA and combined ATRA + MEHP treatments resulted in differential regulation of genes with structural functions in mature Sertoli cells, such as *Cldn11* (Mazaud-Guittot et al., 2011, Mazaud-Guittot et al., 2010), as well as upregulation of canonical retinoic acid receptor target genes, including *Cyp261a, Cyp26c1, Rarb,* and *Stra8* (Fig. 5C-5F). In particular, *Stra8* is a canonical retinoic acid receptor target gene that marks meiosis induction and is considered a hallmark of testicular response to retinoic acid. In addition to *Stra8*, several other DEGs were identified which have well-characterized roles early testis development, such as *Pdgfa*, which is involved in Sertoli cell differentiation and cord development, and *Egr3*, a member of the early growth response family that has previously been cited as a target of phthalates (Brennan and Capel, 2004, Brennan et al., 2003, Gaido et al., 2007) (Fig. 5G, 5H). MEHP, ATRA, and combined exposure to MEHP and ATRA all led to significant differential expression of several genes in the homeobox superfamily, which are implicated in developmental patterning, including upregulation of *Pax2* and downregulation of the canonical RAR target, *Lhx1* (Fig. 5I-J). Additional homeobox superfamily genes that were differentially regulated following combined exposure to MEHP and ATRA included *Rhox8*, *Foxd3*, *Pitx3, Foxr1*, and *Otx2*. Many of these genes were differentially regulated single exposure to MEHP or ATRA. However, combined exposure to MEHP and ATRA had a significantly greater effect on the expression of *Pitx3, Otx2, Pax2*, and *Lhx1* than either treatment alone (Supplemental Tables S1, S3, S6).

MEHP and ATRA enhanced testosterone production

Many prior publications have demonstrated that MEHP reduces testosterone biosynthesis in the rat fetal testis. Because the relatively small number of mouse phthalate studies do not show similar effects on testosterone, here we tested whether in vitro culture with ATRA and/or MEHP would significantly inhibit testosterone production. Media samples from the third day of culture were collected for testosterone analysis. Testosterone biosynthesis in tissue culture media was not significantly influenced by MEHP compared to vehicle. ATRA slightly reduced testosterone, relative to vehicle control, while combined exposure to ATRA and MEHP had an apparently synergistic significant positive effect on testosterone levels, relative to vehicle ($p \leq 0.0001$) (Fig. 6A). In the RNA-seq analysis, expression of genes involved in testosterone biosynthesis followed similar patterns. *Cyp17a1*, *Star*, and *Sbhg* were upregulated in the co-exposure group (Fig. 6B-D). Expression of *Cyp11b1*, a gene that encodes a glucocorticoid biosynthesis enzyme, was reduced following exposure to MEHP and increased following

Table 4
Upstream regulators in IPA analysis of MEHP vs vehicle RNA-seq dataset.

upstream regulator	rank	activation z-score	p-value	target molecules in dataset
RARα	1	2.236	0.03	ATP6V0A4, EGR3, FOXD3, OTX2, STRA8
RARβ	2	2.000	<0.01	ATP6V0A4, FOXD3, OTX2, STRA8
RARγ	3	2.000	0.01	ATP6V0A4, FOXD3, OTX2, STRA8
troglitazone	4	2.000	0.12	ANGPTL4, CIITA, CKM, NR4A3
dexamethasone	13	1.623	0.02	ANGPTL4, CD74, CYP11B2, DCT, EGR3, FOXD3, HLA-DQB1, HLA-DRB5, KRT17, Ly6a (includes others), NR4A3, PCSK9, PDGFA, SHBG, SHH, SLC12A1, SLC25A34, SLC9A3
pioglitazone	14	1.457	<0.01	ANGPTL4, CKM, CYP11B2, NR4A3, SLC9A3
rosiglitazone	35	−0.113	<0.01	ANGPTL4, CIITA, CKM, HMGCS2, SHBG, SLC12A1, SLC9A3, SPN

Upstream regulators predicted by Ingenuity Pathway Analysis (IPA), based on significantly differentially regulated genes in *ex vivo* fetal mouse testes cultured in MEHP. The regulatory molecules that are listed as predicted upstream regulators met the following criteria: activation z score > 2, p-value < 0.05, or both.
7 of the top 35 predicted upstream regulators, ranked by magnitude of activation z-score, including the top 3 predictions, pertained to RAR, PPAR, or GR signaling. The table presents a partial list selected from a total of 375 predicted upstream regulators.

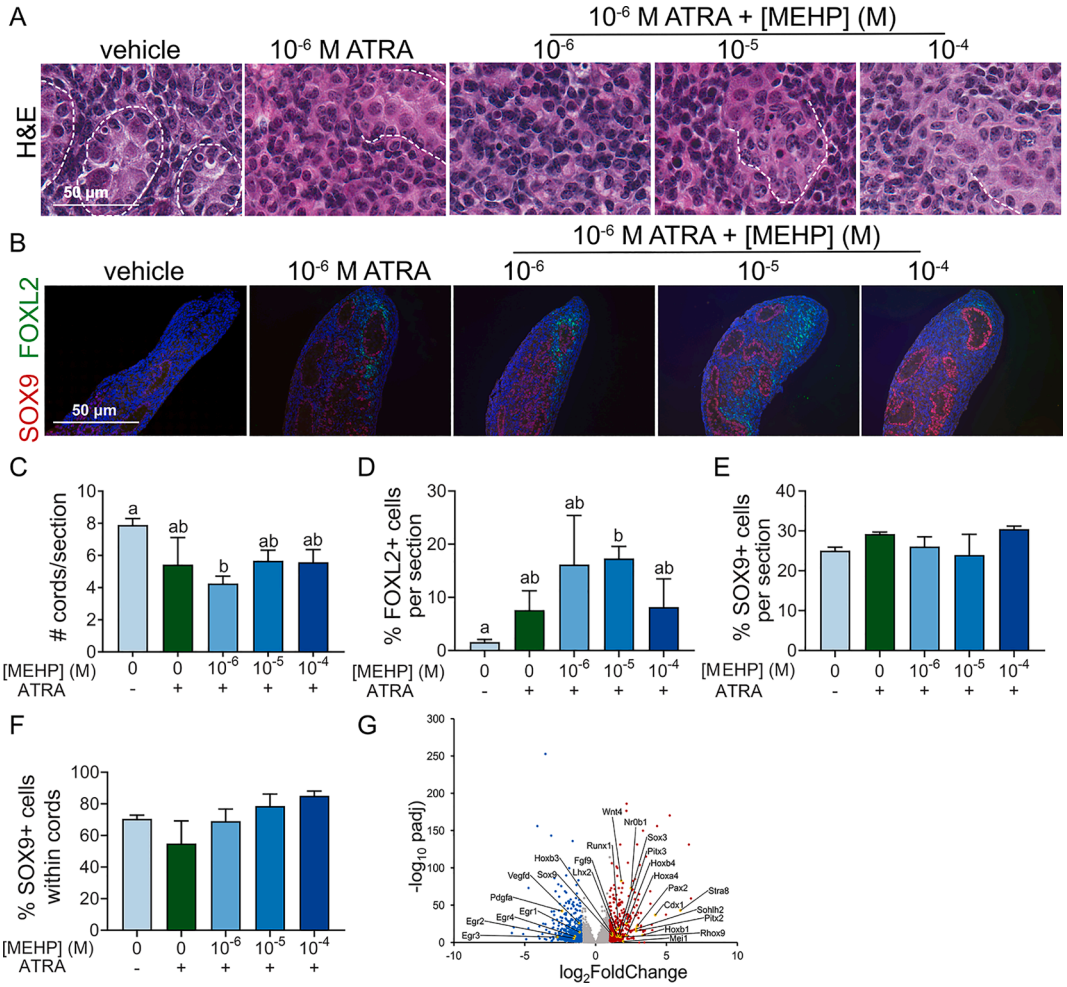

Fig. 4. ATRA and MEHP co-exposure disrupted seminiferous cord development and induced FOXL2 expression in fetal mouse testicular somatic cells. A. Testes exposed to a combination of ATRA and MEHP for 3 days showed a higher level of seminiferous cord disruption than vehicle control. Dashed lines indicate seminiferous cord basement membranes. B. A greater number of FOXL2-positive cells were observed in testes treated with the combination of ATRA and MEHP, relative to vehicle. C. Samples treated with 10^{-6} M ATRA + 10^{-6} M MEHP had a significant reduction in the number of seminiferous cords compared to vehicle control. Bars not connected by the same letter differ significantly by one-way ANOVA followed by Tukey's test ($p < 0.05$), n = 6–7/group and 28 vehicle. D. Testes treated with a combination of 10^{-6} M ATRA and 10^{-5} M MEHP had a significantly increased number of FOXL2-positive cells compared to vehicle control by Kruskal-Wallis test followed by Dunn's multiple test correction ($p < 0.05$). E. SOX9-positive Sertoli cell number varied slightly with no statistically significant changes in total cell count by one-way ANOVA followed by Tukey's test ($p < 0.05$). F. 10^{-6} M ATRA and MEHP-treated samples did not significantly affect the proportion of SOX9-positive cells localized within seminiferous cords by Kruskal-Wallis test followed by Dunn's multiple test correction ($p < 0.05$). For all immunofluorescence analyses, n = 3/group and 13 vehicle. On X-axis labels (C-G), "-" = 0 M ATRA; "+" = 10^{-6} M ATRA. G. Following 1 day in culture, 10^{-6} M ATRA + 10^{-4} M MEHP treatment significantly upregulated 495 genes (red circles) and downregulated 608 genes (blue circles), relative to vehicle control, n = 4 treated and 15 vehicle. Labeled genes are involved in testis development and spatial patterning during development.

exposure to ATRA. However, transcript counts were not significantly changed as a result of MEHP and ATRA combined exposure (Fig. 6E). On the other hand, neither ATRA, MEHP alone nor a combined exposure of both had a significant effect on *Insl3* or *Hsd3b1* expression (Fig. 6F, 6G).

ATRA and MEHP altered mouse fetal testicular germ cell development

Germ cell development depends on development of intact seminiferous cords. Because of the effects of both ATRA and MEHP on cord development, here we tested whether these treatments would alter germ cell development. Exposure of mouse fetal testes to ATRA, MEHP, or a combination of ATRA and MEHP, changed the transcriptional profile for genes related to germ cell development (Fig. 7A, Supplemental Table S9). Gene expression analysis revealed that ATRA significantly differentially regulated the expression of 231 germ cell development genes that were identified in a recent single-cell RNA-seq publication (Zhao et al., 2021). Specifically, ATRA upregulated genes first expressed during germ cell development stages, including peaks of DEGs associated with the quiescent prospermatogonia, differentiating and differentiated spermatogonia, and pachytene spermatocyte stages. Conversely, out of 44 germ cell-specific DEGs, MEHP downregulated more genes first expressed during the quiescent pro-spermatogonia stage and pachytene stage than it upregulated. Combined exposure to MEHP and ATRA resulted in 497 germ-cell specific DEGs with peaks at the same stages as ATRA, but with a greater number of downregulated genes in the quiescent prospermatogonia and pachytene spermatocyte gene clusters. Although these gene expression data demonstrate that both ATRA and MEHP had effects on germ cell development, only 10^{-6} M ATRA significantly reduced germ cell count. Neither MEHP nor the ATRA + MEHP combined exposure significantly altered germ cell count, but both treatments showed a slightly lower mean germ cell count (Fig. 7B-E). Because phthalates are known to induce MNGs, we counted MNGs in histological sections stained with H&E. No treatment significantly induced MNGs, relative to vehicle control, in the present study

Table 5
Top 11 GO terms obtained by GO term enrichment analysis of ATRA + MEHP vs vehicle RNA-seq dataset.

GO ID	GO biological process	% significant genes	p-adj
GO:0007275	multicellular organism development	8.53	0.009
GO:0009952	anterior/posterior pattern specification	16.96	0.016
GO:0051965	positive regulation of synapse assembly	21.13	0.016
GO:0071300	cellular response to retinoic acid	25	0.026
GO:0071805	potassium ion transmembrane transport	17.78	0.026
GO:0048791	calcium ion-regulated exocytosis of neurotransmitter	32.14	0.026
GO:0010466	negative regulation of peptidase activity	15.52	0.032
GO:0048704	embryonic skeletal system morphogenesis	21.43	0.032
GO:0017158	regulation of calcium ion-dependent exocytosis	32	0.044
GO:0030154	cell differentiation	8.13	0.047
GO:0007613	memory	17.28	0.047

Abbreviations: DR = significantly differentially regulated, GO = gene ontology, p-adj = multiplicity adjusted p-value. Summary of significantly enriched GO terms in combined ATRA + MEHP exposure versus vehicle control. The percent of significant genes indicates the percent of enriched genes within GO terms, where significance of the enriched term has a q-value of < 0.04. Full results are reported in Supplemental Table S7.

(Supplemental Fig. S1).

Discussion

The goal of this study was to test the hypothesis that disruption of RA signaling contributes to fetal testicular toxicity of the phthalate, MEHP. Phthalates are ubiquitous xenobiotics that disrupt male gonad development, causing a phenotype called testicular dysgenesis in the rat (Mitchell et al., 2012). Although phthalate toxicity is better described in the rat than the mouse, the effects of phthalates on mouse testicular development are similar, including disrupted seminiferous cord morphogenesis and induction of MNGs (Gaido et al., 2007, Heger et al., 2012, Boekelheide et al., 2009, Kleymenova et al., 2005). In our previous study, we found that ATRA and MEHP interacted in cultured fetal rat testes, having opposite effects on seminiferous cord morphogenesis (Spade et al., 2019b). In the present study, we report that ATRA altered seminiferous cord morphogenesis in the fetal mouse testis by changing testicular supporting cell differentiation and localization, and that MEHP enhanced these effects of ATRA. Both treatments significantly altered expression of genes related to testis development, and neither compound significantly reduced testosterone. These results support the hypothesis that RA signaling is disrupted by phthalate exposure, contributing to the effect of phthalates on seminiferous cord development. In testes cultured in media containing a combination of ATRA and MEHP, the addition of MEHP enhanced the degree to which ATRA disrupted seminiferous cord development, providing strong evidence of an interaction between ATRA and MEHP. In contrast, three days of culture in media containing $10^{-6} - 10^{-4}$ M MEHP alone did not cause significant changes to seminiferous cord development in GD 14 mouse testes. It is notable that the dose–response in the combined exposure to MEHP and ATRA was non-monotonic (Fig. 4), as we previously reported in the rat, suggesting that the influence of MEHP on RA signaling is potentially indirect and that the effect could be subject to negative feedback at high phthalate concentrations. It is also notable that the significant effect in the co-exposure experiment in this study was in the opposite direction from our prior study in the rat. Here, a low or moderate concentration of MEHP decreased seminiferous cord number and increased FOXL2-positive cell count beyond the level imparted by ATRA alone (Fig. 4), while in the rat, the addition of MEHP antagonized the effect of ATRA on cord number (Spade et al., 2019b). The present study does not provide conclusive evidence of the mechanism by which MEHP can influence RA signaling. However, it is likely that phthalate toxicity mechanism is multifactorial and involves multiple signaling processes, including disrupted RA signaling.

We found further evidence of an interaction between MEHP and RA signaling in our RNA-seq analysis, in which there was a considerable intersection of DEGs between MEHP and ATRA, including many DEGs involved in testis morphogenesis and spatial patterning. Previous publications have reported that MEHP alters the ATRA-dependent activation of RARA in cultured mouse fetal Sertoli cells, presumably because MEHP binds to PPARs, leading to competition for RXR between RARs and PPARs (Dufour et al., 2003, Bhattacharya et al., 2005). Because RAR and PPAR signaling are directly mediated by changes in gene expression, we performed whole-transcriptome RNA-seq analysis to investigate whether MEHP and ATRA have similar gene expression effects in the mouse fetal testis. Our RNA-seq analysis revealed that over half of the genes that were differentially regulated by MEHP were also differentially regulated by ATRA, including 5 canonical RAR target genes, *Pdgfa*, *Otx2, Stra8*, *Lhx1* and *Slac9a2* (Fig. 5). This is further evidence that MEHP influences retinoic acid signaling, but the nature of this interaction is not clear from our results. Although the prior evidence suggests a competitive interaction between MEHP and ATRA (Dufour et al., 2003), in almost all cases, the direction of gene expression regulation by MEHP and ATRA in the present study was the same. In the co-exposure gene expression analysis, the effect of ATRA and MEHP appeared to be approximately additive for some genes, such as *Lhx1*, *Egr3*, and *Pdgfa* (Fig. 5), while some genes had a greater than additive gene expression pattern consistent with synergism between ATRA and MEHP, such as *Rarb*, *Stra8*, *Pax2*, *Cyp26a1*, and *Cyp26c1* (Fig. 5). Only the corticosteroid biosynthesis gene, *Cyp11b1*, was regulated in opposite directions by ATRA and MEHP, resulting in no significant net effect in the combined exposure. Our gene expression analysis was also consistent with prior reports with respect to the mechanism by which ATRA alters testis development. Our findings included dysregulation of *Wnt4*, *Foxl2*, and *Nr0b1* expression in both the ATRA and combined exposure groups (Supplemental Tables S3, S6). This is consistent with our previous findings in cultured rat testes treated with ATRA (Spade et al., 2019a), as well as an experiment in which mouse fetal testes were cultured with an ATRA analogue or a CYP26 inhibitor (Bowles et al., 2018).

In this study, as in previous experiments involving phthalate exposure in fetal mice, MEHP did not suppress fetal Leydig cell function. Although phthalates reduce testosterone levels in the rat fetal testis (Hannas et al., 2011a, Howdeshell et al., 2015, Howdeshell et al., 2008, Veeramachaneni and Klinefelter, 2014), some effects of phthalates on seminiferous cord morphogenesis are consistent across the human, mouse, and rat fetal testis, and apparently occur through androgen-independent mechanisms (Gaido et al., 2007, Spade et al., 2014, Heger et al., 2012, Lambrot et al., 2009, Mitchell et al., 2012). We previously reported that ATRA ablated seminiferous cord formation in the rat fetal testis and that MEHP antagonized this effect of ATRA, and that both treatments and the combined exposure reduced testicular testosterone (Spade et al., 2019a, Spade et al., 2019b). On the contrary, in the present study, MEHP and ATRA in combination caused an increase in testosterone production and gene expression effects consistent with that increase. MEHP differentially regulated the expression of two genes involved in cholesterol biosynthesis, *Mvd* and *Hmgcs2*, as well as the mitochondrial cholesterol transport gene, *Star*, which is a

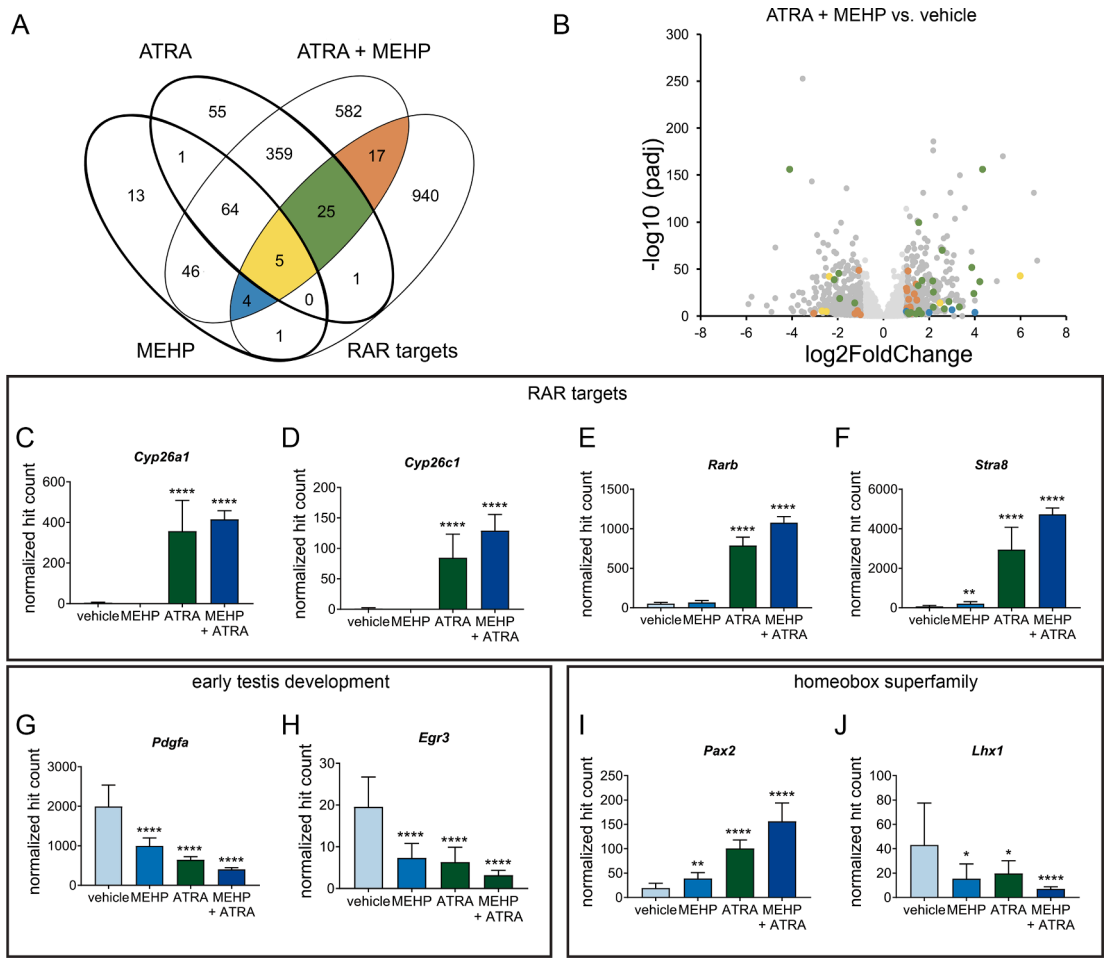

Fig. 5. MEHP altered expression of numerous ATRA target genes and testis development genes following 1 day of culture. A. Analysis of common DEGs among 510, 134, and 1102 genes that were differentially expressed following exposure to 10^{-6} M ATRA, 10^{-4} M MEHP, and 10^{-6} M ATRA + 10^{-4} M MEHP, respectively, relative to vehicle, based on RNA-seq statistical analysis by DESeq2 described in Figs. 1, 2, and 4. 70 of the 134 MEHP differentially regulated genes were also differentially regulated by ATRA (52.2 % shared differentially regulated genes, illustrated by thick lines in Venn diagram). Further, 120 of 134 MEHP differentially regulated genes were also differentially regulated in the MEHP + ATRA combined exposure. 51 of the genes that were differentially regulated by at least one treatment are characterized RAR target genes (Balmer and Blomhoff, 2002), labeled as "RAR targets" and illustrated by the colored overlap areas. B. ATRA + MEHP vs vehicle volcano plot highlighting differentially regulated genes that are characterized RAR target genes. Colored circles correspond to the overlap areas in panel A. C-F. MEHP alone had no effect on the expression of the majority of canonical RAR signaling targets, but induced expression of the RAR target and meiosis gene, *Stra8*. However, when combined with ATRA, MEHP synergistically enhanced the effect of ATRA on the expression of numerous canonical RAR target genes, including *Cyp26a1, Cyp26c1, Rarb,* and *Stra8*. G and H. Among common differentially regulated genes, MEHP, ATRA, and the combined exposure additively decreased the expression of early testis development genes, *Egr3* and *Pdfga*. I and J. MEHP and ATRA had additive effects on the expression of homeobox superfamily genes, including *Pax2* (upregulated) and *Lhx1* (downregulated), indicating a possible mechanism by which both treatments might influence developmental patterning.

component of the protein complex that is responsible for the transport of cholesterol from the outer to the inner mitochondrial membrane during testosterone biosynthesis. *Star* expression was significantly up-regulated by ATRA compared to the control group, and combined exposure to ATRA and MEHP increased *Star* expression, relative to both the ATRA and control treatment groups (Fig. 6). Among testosterone biosynthesis genes, *Hsd3b1* expression was not significantly altered by any treatment, but *Cyp17a1* expression was significantly up-regulated by the combined exposure to ATRA and MEHP, relative to vehicle control. Finally, we observed an increase in *Shbg* expression in all treatment groups. *Shbg* codes for the sex hormone binding globulin, SHBG, which binds approximately 50 % of circulating testosterone in humans. One previous study in human neonates found that expression of *Shbg* was associated with certain phthalate metabolites (Main et al., 2006). Increased *Shbg* and testosterone is consistent with the clinical effect of PPARγ agonist, Rosiglitazone (Kapoor et al., 2008, Hammond, 2011), which further suggests a role for PPARγ in phthalate toxicity. Our results are consistent with published reports that testosterone and SHBG engage in bidirectional regulation, in which elevated testosterone can cause an increase in *Shbg* expression and elevated SHBG can lead to reduced free testosterone, increased LH release, and increased testosterone biosynthesis (Laurent et al., 2016a, Laurent et al., 2016b). However, the mechanism by which testosterone regulates *Shbg* expression is unknown (Hammond, 2011). Insulin-like growth factor3 (*Insl3),* which is also expressed in Leydig cells, has a well characterized role in the second phase of testicular descent (Bogatcheva and Agoulnik, 2005, Nef and Parada, 1999). Unlike testosterone levels, *Insl3* gene expression was not affected by any treatment. Notably, we measured gene expression on day 1 of culture and testosterone on day 3 of culture. As in our previous publication studying the rat fetal testis in the same model system, there was consistency between steroid hormone-related gene expression changes measured on day 1 and testosterone levels measured on day 3 of culture (Spade et al., 2019b).

Both ATRA and MEHP altered the expression of genes that contribute to essential early testicular morphogenesis functions. One gene that was differentially regulated by both treatments was *Pdgfa*, which encodes for

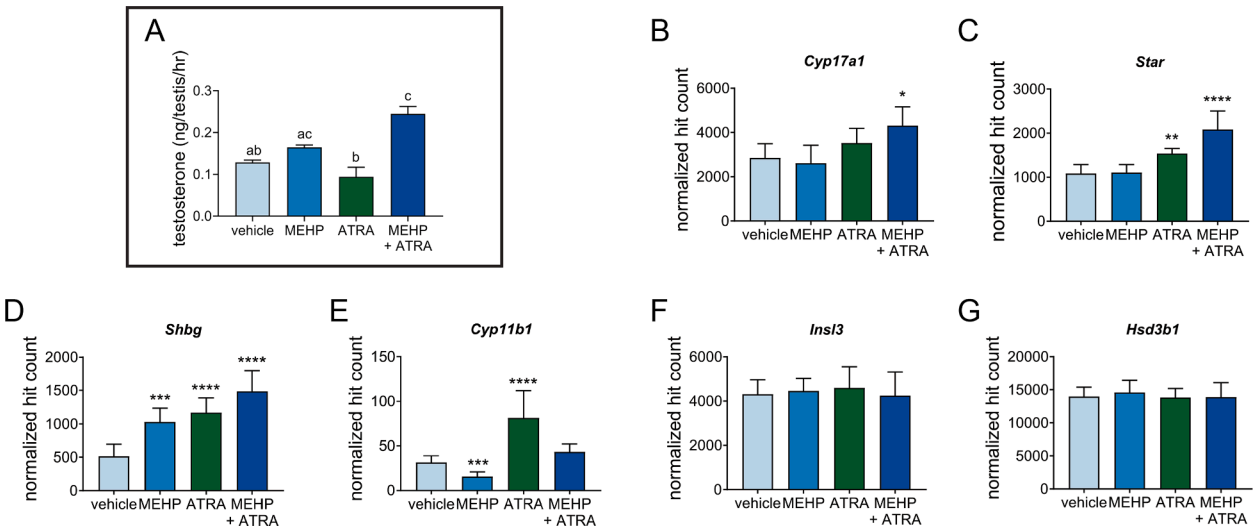

Fig. 6. MEHP and ATRA co-exposure significantly increased testosterone production in *ex vivo* testis cultures. A. Combined exposure to 10^{-6} M ATRA and 10^{-4} M MEHP significantly increased testosterone secretion into tissue culture media that was collected on day 3 of culture, compared to ATRA and vehicle control. Bars not connected by the same letter differ significantly by Kruskal-Wallis test followed by Dunn's multiple test correction ($p < 0.05$), n = 7/treatment group and 21 vehicle. This was consistent with gene expression findings related to Leydig cell function and testosterone biosynthesis. B-C. Among testosterone biosynthesis genes, the combined exposure increased *Cyp17a1* expression, and MEHP enhanced the effect of ATRA on *Star* expression. D. MEHP and ATRA combined exposure resulted in a significant additive effect on *Shbg* expression. E. MEHP and ATRA had opposite effects on the expression of the corticosteroid biosynthesis gene, *Cyp11b1*. F-G. Neither ATRA nor MEHP significantly altered the expression *of Insl3* or *Hsd3b1*. Panels B-G based on RNA-seq statistical analysis by DESeq2 for samples cultured with DMSO, 10^{-6} M ATRA, 10^{-4} M MEHP, and combined exposure of 10^{-6} M ATRA and 10^{-4} M MEHP for 1 day, described in Figs. 1, 2, and 4.

platelet-derived growth factor (PDGF) alpha. It is well-known that PDGF signaling is required for normal testis development, and in experiments in which the PDGF receptor, *Pdgfra* is knocked out, the testicular vasculature does not form properly or guide the development of seminiferous cords correctly (Coveney et al., 2008, Cool et al., 2011, Brennan et al., 2003). Another gene differentially regulated by both ATRA and MEHP was *Egr3*, a member of the immediate-early growth response family of zinc-finger proteins involved in early development. Although *Egr3* has no characterized role in the XY gonad, *Egr1* and *Egr4* play vital roles in male fertility in the mouse (Tourtellotte et al., 1999, Lei and Heckert, 2002). Previously, *Egr1* and *Egr2* were identified as key gene expression targets of di-*n*-butyl phthalate in the rat fetal testis (Johnson et al., 2007). Beyond the single gene approach, MEHP vs vehicle enrichment analysis of Gene Ontology Biological Processes (Table 3) identified the term "structure formation and morphogenesis" as an enriched category. Genes within that category included *Nodal, Shh,* and *Grem1*, which were all downregulated by MEHP. These genes also have well-characterized roles in the development of mouse and human Sertoli cells (Tian et al., 2015, Wu et al., 2013, Jørgensen et al., 2018), testicular angiogenesis (Mitola et al., 2010), and seminiferous cord formation (Clark et al., 2000, Franco and Yao, 2012). Inappropriate activation of *Shh* in E13.5 fetal mouse testis has been shown to cause defects in testis cord formation (Lee et al., 2011). In addition to genes with well-characterized roles in early testis development, MEHP significantly altered the expression of seven genes in the homeobox superfamily, which are regulators of developmental patterning, including *Rhox8, Foxd3, Pitx3, Foxr1, Otx2, Pax2,* and *Lhx1*. While several of these genes do not have currently characterized roles in testis development, *Pax2* has a well-established role in the development of the Wolffian duct, a precursor of epididymis, vas deferens, and seminal vesicles (Torres et al., 1995). *Rhox8* is exclusively expressed in Sertoli cells within the fetal testis, and its ablation leads to impaired fertility and reduced expression of *Sox9* and *Sox8*, which are crucial genes for Sertoli cell identity and functionality (Daggag et al., 2008, Welborn et al., 2015).

Taken together, this analysis provides strong evidence that MEHP alters the expression of genes that regulate cellular differentiation and pattern formation in the fetal testis. Phthalates have been consistently shown to reduce testosterone biosynthesis in the rat fetal testis (Hannas et al., 2011a, Howdeshell et al., 2015, Howdeshell et al., 2008, Mylchreest et al., 2002, Gray et al., 2000, Furr et al., 2014). However, the effects of MEHP in the present study are independent of reduced testosterone, as evidenced by the lack of effect of MEHP on testosterone levels and the increase in testosterone in the cultures that were treated with both ATRA and MEHP (Fig. 6). This observation is consistent with prior studies on mice and in human fetal testis xenotransplants, in which phthalates induced MNGs or caused seminiferous cord malformation through androgen-independent mechanisms (Spade et al., 2014, Heger et al., 2012, Lambrot et al., 2009, Mitchell et al., 2012), Several recent reviews, including our own, have proposed mechanisms or adverse outcome pathways to describe the events that are involved in phthalate toxicity (Howdeshell et al., 2015, Conley et al., 2018, Clewell et al., 2020, Arzuaga et al., 2020, Gray et al., 2020, Li and Spade, 2021). We believe that the data generated by the present study, when analyzed in the context of previous papers that investigated phthalate toxicity in mouse, rat, and human fetal testis, strongly suggest that phthalates have either a single mechanistic target upstream of developmental and function of both Sertoli and Leydig cells, or a primary target in the Sertoli cell that adversely affects Leydig cell function in the rat in a manner that is not reproduced in the mouse.

Our data indicate that one of the effects of disrupting RA signaling in the fetal testis is altered Sertoli cell differentiation and seminiferous cord development. *Sox9* is required for continuous commitment to testis development. In the absence of *Sry* and *Sox9*, supporting cells commit to a granulosa cell phenotype and express *Foxl2* (Kashimada et al., 2011, Bowles et al., 2018). Supporting cell phenotype is labile and can be influenced by genetic and environmental manipulations (Nicol and Yao, 2015, Raymond et al., 2000). Disruption of the fetal testicular RA concentration disrupts fetal testicular development and induces germ cell death (Bowles et al., 2006, MacLean et al., 2007, Spade et al., 2019a). Our previous work on rat testes demonstrated that phthalates interfere with RA signaling, disrupting Sertoli cell development and seminiferous cord formation (Spade et al., 2019a, Spade et al., 2019b). Here we show that in the mouse, similar to the rat fetal testis, exogenous ATRA triggers the expression of FOXL2 in mouse testicular somatic cells. MEHP did not

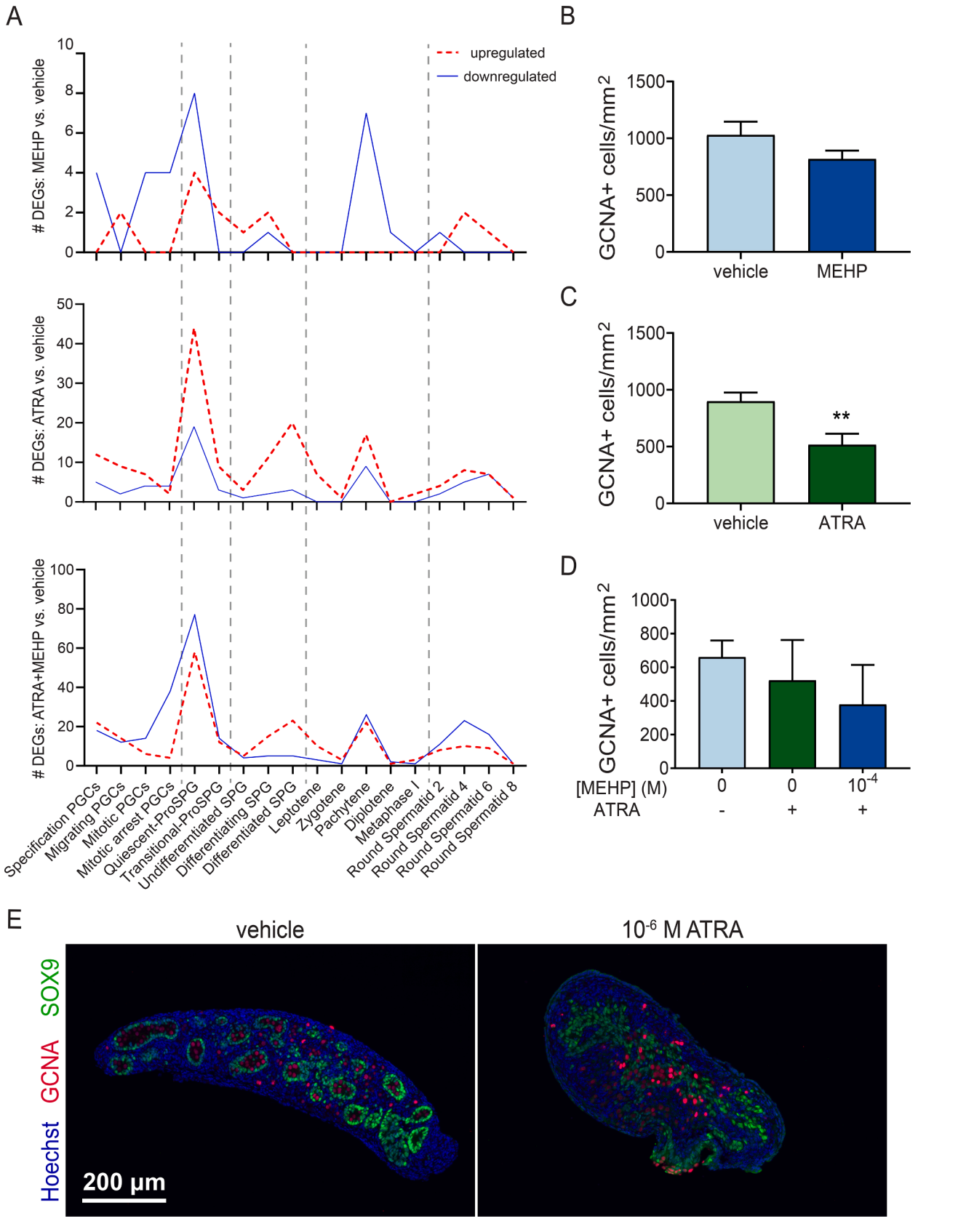

(caption on next page)

Fig. 7. ATRA and MEHP altered the transcriptional profile of genes first expressed during germ cell development stages. A. Germ cell-specific gene expression clusters were extracted from Zhao et al. (2021), and are displayed on the x-axis in order of developmental stage. DEG lists for each of the three RNA-seq analyses reported in this paper (MEHP vs vehicle, ATRA vs vehicle, and MEHP + ATRA vs vehicle) were searched for genes first expressed in any germ cell RNA-seq cluster, and the number of genes up- or downregulated per cluster is displayed on the chart. ATRA exposure resulted in upregulation of genes that are first expressed during developmental stages of greatest germ cell differentiation, including quiescent spermatogonia, differentiating and differentiated spermatogonia, and pachytene spermatocyte stages. MEHP exposure resulted in a larger number of downregulated than upregulated genes first expressed in quiescent prospermatogonia and pachytene spermatocytes in the single-cell RNA-seq dataset. The MEHP + ATRA comparison resulted in differential regulation peaks in many of the same stages as each of the single exposures. B. 10^{-4} M MEHP did not significantly reduce germ cell count by unpaired *t*-test, n = 7 for MEHP and vehicle. C. 10^{-6} M ATRA significantly decreased germ cell count, relative to vehicle control. ** $p < 0.001$ by unpaired *t*-test, n = 8 for ATRA and vehicle. D. 10^{-6} M ATRA alone or in combination with 10^{-4} M MEHP did not significantly reduce GCNA-positive cell count in the combined exposure experiment by one-way ANOVA followed by Tukey's multiple comparisons test ($p < 0.05$), n = 3/ treatment group and 6 vehicle. E. Representative images of cultured testes treated with vehicle and 10^{-6} M ATRA, showing the reduced number of germ cells per section following ATRA exposure.

significantly change the identity of *Sox9*-positive supporting cells through the induction of FOXL2. However, MEHP in combination with ATRA enhanced the expression of FOXL2 above the level induced by ATRA alone. In addition to altering supporting cell fate, ATRA and the combined exposure to ATRA and MEHP disrupted the localization of *Sox9*-positive Sertoli cells, leading to a reduced proportion of seminiferous cord-associated Sertoli cells (Fig. 1F, 4F). The gene expression analysis suggests that this occurs because of disrupted expression of Sertoli and granulosa cell identity genes. ATRA and the ATRA + MEHP co-exposure treatment caused a significant upregulation in the expression of genes involved in ovarian development including, *Foxl2, Runx1, Fstl3, Wnt4, Sohlh2, Nr0b1, Mei1, and Rhox9*, which suggests a shift toward ovarian supporting cell developmental pathways in these fetal testis cultures (Nicol et al., 2018, Nicol et al., 2019, Ottolenghi et al., 2007). Furthermore, data showed a significant upregulation of *Sox3*. *Sox3* has sexually dimorphic functions in male and female somatic cells, and loss of *Sox3* leads to disruption of seminiferous tubules and aberrant germ cell development in XY gonads (Weiss et al., 2003). In immunofluorescent experiments, we did not observe cells expressing both SOX9 and FOXL2 simultaneously, although SOX9-positive and FOXL2-positive cells were often in close proximity (Fig. 1). This suggests that that FOXL2 expression likely did not occur due to trans-differentiation of Sertoli cells into granulosa-like cells, although this can occur in genetic mutants (Nicol et al., 2018). We also did not observe a decrease in SOX9-positive cells, which might suggest dedifferentiation of Sertoli cells prior to expression of FOXL2. More likely, the increase in FOXL2 expression following exposure to exogenous ATRA occurred because of *de novo* differentiation of undifferentiated supporting cells. This suggests that the mechanism by which ATRA and MEHP disrupt spatial patterning of testicular cords involves disruption of Sertoli cell localization rather than loss of Sertoli cell identity in differentiated Sertoli cells.

The majority of the experiments reported in this paper focus on testicular somatic cells and seminiferous cord development. However, our findings indicated that both ATRA and MEHP altered mouse fetal testicular germ cell development, consistent with previous publications in similar model systems (Trautmann et al., 2008, Muczynski et al., 2012). Our analysis of GCNA data indicated that ATRA significantly reduced the number of germ cells compared to vehicle control, while MEHP and the combination of ATRA and MEHP did not significantly reduce germ cell count (Fig. 7). The mechanism by which ATRA alters germ cell development is well-described. It is known that ATRA induces germ cell differentiation and meiosis (Bowles and Koopman, 2007, Koubova et al., 2014, Koubova et al., 2006), which is likely to be detrimental to germ cells that are not competent for meiosis. Beyond germ cell survival, to determine whether ATRA and MEHP altered germ cell function and development, we compared the lists of DEGs from our RNA-seq analysis with a list of male germ cell genes and the stages of development when they are first expressed from a recent single-cell RNA-seq study (Zhao et al., 2021) (Fig. 7). This comparison revealed that ATRA exposure resulted in upregulation of genes that are first expressed during germ cell differentiation stages, namely the quiescent prospermatogonia, differentiating and differentiated spermatogonia, and pachytene spermatocyte clusters. In contrast, MEHP exposure downregulated more genes associated with the quiescent prospermatogonia and pachytene gene clusters than it upregulated, suggesting that ATRA and MEHP have opposing effects on expression of genes associated with these two germ cell differentiation stages. Several caveats should be noted. First, all gene expression data generated by our RNA-seq analyses are from samples cultured on GD14, when germ cells are most likely in the prospermatogonia stage. Therefore, expression of genes from subsequent developmental clusters is likely aberrant for this stage. Second, some genes in the single-cell RNA-seq dataset are likely to be expressed in other cell types in the whole testis, so our bulk RNA-seq analysis is not strictly limited to germ cell gene expression. Finally, while single-cell RNA-seq provides cell type specificity, it does not provide the same sensitivity for low-expression genes as bulk RNA-seq, so some genes may normally be expressed earlier than they appear in the single-cell clusters. In spite of these limitations, the result of our analysis was consistent with prior reports that ATRA induces germ cell differentiation, as well as the knowledge that MEHP prolongs the expression of pluripotency genes including *Oct4* (Jobling et al., 2011).

A commonly reported effect of phthalates on the fetal testis is induction of MNGs. *In utero* phthalate exposure has consistently induced MNGs in rats and mice, and this has been replicated in human fetal testis xenotransplant studies (Li and Spade, 2021). In testis culture experiments, MEHP has been reported to induce MNGs in cultured GD 15 and GD 18 mouse testes, as well as cultured GD 20 and PND 3 rat testes (Boisvert et al., 2016, Lehraiki et al., 2009). Therefore, it could reasonably be supposed that MEHP exposure in the present study would induce MNGs. However, no treatment resulted in significant induction of MNGs, relative to the vehicle control (Supplemental Fig. S1). It is likely that the gestational age at which we initiated our cultures is not sensitive to MNG induction in mice. To our knowledge, the earliest day on which cultured mouse testes are sensitive to induction of MNGs is GD 15 (Lehraiki et al., 2009). This is consistent with our and other groups' previous reports that the window of sensitivity for MNG induction in the rat coincides with the quiescent prospermatogonia stage beginning on GD 18 (Spade et al., 2015, Ferrara et al., 2006), given that the quiescent stage begins around GD 16 in the mouse (Culty, 2009).

There is also extensive evidence from prior publications that phthalates alter Sertoli cell function, and it can be presumed that some of the effects of phthalates on germ cells are secondary to Sertoli cell effects. In particular, phthalates disrupt the Sertoli cell cytoskeleton in ways that are likely detrimental to germ cells, including the loss of vimentin and retraction of Sertoli cell cytoskeletal processes (Fisher et al., 2003, Kleymenova et al., 2005, Spade et al., 2014). In our gene expression analysis of MEHP-treated vs vehicle-treated mouse testes, GO terms related to cell–cell junctions were not significantly enriched. However, some genes classified under these GO terms were significantly differentially expressed, including *Plxnb3*, *Nodal*, and *Mpzl2* (Supplemental Table S4). *Nodal* in particular is a vital component of Sertoli cell-Germ cell interaction during fetal testis development (Jørgensen et al., 2018, Tian et al., 2015, Wu et al., 2013). Similarly, in the ATRA vs vehicle RNA-seq analysis, GO terms associated with cell–cell adhesion were not significantly enriched, but several genes that fall under these terms were significantly differentially expressed, including *Wnt4*,

Plxnb3, *Muc4*, and *Fstl3*. Changes in expression of genes involved in cell–cell interaction could be involved in the mechanisms by which MEHP and ATRA alter seminiferous cord integrity and Sertoli cell-germ cell contacts, and these significant DEGs are candidates for further study.

Despite the evidence of an interaction between MEHP and ATRA, it is not clear that phthalates directly interact with retinoic acid receptors. Phthalates are known to act as ligands for peroxisome proliferator activated receptors (PPARs). Presently, no evidence has been published to demonstrate that activation of PPARα is involved in the mechanism of phthalate toxicity in the testis (Hannas et al., 2012). However, binding of MEHP to RXRs, which form heterodimers with RARs and PPARs, or binding of MEHP to PPARs could lead to crosstalk with RA signaling. It has been previously demonstrated in cultured mouse Sertoli cells that MEHP can influence RA signaling by inhibiting RARα translocation into the nucleus as a result of competition for RXR between ligand-activated RARs and PPARs (Bhattacharya et al., 2005, Dufour et al., 2003). Additionally, one in silico analysis predicted that phthalates could bind to both PPARs and RXRs (Sarath Josh et al., 2014). Our present data also suggest that phthalates are capable of influencing retinoic acid and PPAR signaling in the testis, based on differential expression of RAR and PPAR target genes by MEHP. Finally, it has previously been demonstrated that dexamethasone, a glucocorticoid receptor (GR) agonist, enhances phthalate toxicity (Leng et al., 2020, Zhang et al., 2019). Consistent with the hypothesis that nuclear receptor crosstalk is a component of phthalate toxicity, our IPA analysis identified three RAR isoforms, three PPARγ ligands and dexamethasone, the GR agonist, as putative upstream regulators of the MEHP gene expression response (Table 4, Fig. 3). Future studies will aim to dissect the mechanisms of these nuclear receptor signaling pathway interactions.

Conclusion

The results of this study support the hypothesis that MEHP exposure disrupts RA signaling in the fetal testis. MEHP enhanced the adverse effect of ATRA on structural development of the fetal mouse testis. The two compounds individually differentially regulated many genes, 70 of which were altered by both treatments, suggesting possible pathways that mediate this interaction. Because MEHP is a known PPAR ligand, crosstalk between two nuclear receptor signaling pathways, RA signaling and PPAR signaling, might explain the interaction between MEHP and ATRA. This suggests a role for disruption of RA signaling in the mechanisms of MEHP-induced fetal testicular toxicity.

Funding

This work was funded by the National Institute of Environmental Health Sciences [R00ES025231]. Maha Alhasnani received funding from the Saudi Arabian Cultural Mission (SACM) and King Abdulaziz University (KAU). The University of Virginia Center for Research in Reproduction Ligand Assay and Analysis Core is supported by the Eunice Kennedy Shriver NICHD/NIH [R24HD102061]. The funders had no role in study design; in the collection, analysis, and interpretation of data; in the writing of the report; or in the decision to submit the article for publication.

CRediT authorship contribution statement

Maha A. Alhasnani: Conceptualization, Methodology, Investigation, Formal analysis, Writing – original draft, Writing – review & editing. **Skylar Loeb:** Conceptualization, Methodology, Investigation, Formal analysis, Writing – original draft, Writing – review & editing. **Susan J. Hall:** Methodology, Investigation, Writing – review & editing. **Zachary Caruolo:** Methodology, Investigation, Writing – review & editing. **Faith Simmonds:** Investigation, Formal analysis, Writing – review & editing. **Amanda E. Solano:** Investigation, Formal analysis, Writing – review & editing. **Daniel J. Spade:** Conceptualization, Investigation, Formal analysis, Writing – review & editing, Writing – original draft.

Declaration of Competing Interest

The authors declare the following financial interests/personal relationships which may be considered as potential competing interests: Daniel Spade reports a relationship with National Toxicology Program that includes: consulting or advisory. Nothing else to disclose.

Data availability

Raw and normalized RNA-seq data are available from the NCBI Gene Expression Omnibus database (Series GSE195969). All other data will be made available upon request.

Acknowledgements

The authors would like to thank Dr. Richard Freiman for generously providing feedback on the manuscript. We would like to thank Paula Weston, Melinda Ankerman, and David Silverberg for the processing of histological samples.

Appendix A. Supplementary data

Supplementary data to this article can be found online at https://doi.org/10.1016/j.crtox.2022.100087.

References

Albro, P.W., 1986. Absorption, metabolism, and excretion of di(2-ethylhexyl) phthalate by rats and mice. Environ. Health Perspect. 65, 293–298.
Arzuaga, X., Walker, T., Yost, E.E., Radke, E.G., Hotchkiss, A.K., 2020. Use of the Adverse Outcome Pathway (AOP) framework to evaluate species concordance and human relevance of Dibutyl phthalate (DBP)-induced male reproductive toxicity. Reprod. Toxicol. 96, 445–458.
Balmer, J.E., Blomhoff, R., 2002. Gene expression regulation by retinoic acid. J. Lipid Res. 43, 1773–1808.
Benjamin, S., Pradeep, S., Josh, M.S., Kumar, S., Masai, E., 2015. A monograph on the remediation of hazardous phthalates. J. Hazard. Mater. 298, 58–72.
Bhattacharya, N., Dufour, J.M., Vo, M.N., Okita, J., Okita, R., Kim, K.H., 2005. Differential effects of phthalates on the testis and the liver. Biol. Reprod. 72, 745–754.
Boekelheide, K., Kleymenova, E., Liu, K., Swanson, C., Gaido, K.W., 2009. Dose-dependent effects on cell proliferation, seminiferous tubules, and male germ cells in the fetal rat testis following exposure to di(n-butyl) phthalate. Microsc. Res. Tech. 72, 629–638.
Bogatcheva, N.V., Agoulnik, A.I., 2005. INSL3/LGR8 role in testicular descent and cryptorchidism. Reprod Biomed Online 10, 49–54.
Boisvert, A., Jones, S., Issop, L., Erythropel, H.C., Papadopoulos, V., Culty, M., 2016. In vitro functional screening as a means to identify new plasticizers devoid of reproductive toxicity. Environ. Res. 150, 496–512.
Bowles, J., Knight, D., Smith, C., Wilhelm, D., Richman, J., Mamiya, S., Yashiro, K., Chawengsaksophak, K., Wilson, M.J., Rossant, J., Hamada, H., Koopman, P., 2006. Retinoid signaling determines germ cell fate in mice. Science 312, 596–600.
Bowles, J., Feng, C.W., Ineson, J., Miles, K., Spiller, C.M., Harley, V.R., Sinclair, A.H., Koopman, P., 2018. Retinoic acid antagonizes testis development in mice. Cell Rep 24, 1330–1341.
Bowles, J., Koopman, P., 2007. Retinoic acid, meiosis and germ cell fate in mammals. Development 134, 3401–3411.
Brennan, J., Capel, B., 2004. One tissue, two fates: molecular genetic events that underlie testis versus ovary development. Nat. Rev. Genet. 5, 509–521.
Brennan, J., Tilmann, C., Capel, B., 2003. Pdgfr-alpha mediates testis cord organization and fetal Leydig cell development in the XY gonad. Genes Dev. 17, 800–810.
Chen, Y., Reese, D.H., 2016. Disruption of retinol (vitamin A) signaling by phthalate esters: SAR and mechanism studies. PLoS ONE 11, e0161167.
Clark, A.M., Garland, K.K., Russell, L.D., 2000. Desert hedgehog (Dhh) gene is required in the mouse testis for formation of adult-type Leydig cells and normal development of peritubular cells and seminiferous tubules. Biol. Reprod. 63, 1825–1838.
Clewell, R.A., Leonard, J.A., Nicolas, C.I., Campbell, J.L., Yoon, M., Efremenko, A.Y., McMullen, P.D., Andersen, M.E., Clewell, H.J., Phillips, K.A., Tan, Y.-M., 2020. Application of a combined aggregate exposure pathway and adverse outcome pathway (AEP-AOP) approach to inform a cumulative risk assessment: A case study with phthalates. Toxicol. In Vitro 66, 104855.
Conley, J.M., Lambright, C.S., Evans, N., Cardon, M., Furr, J., Wilson, V.S., Gray Jr., L.E., 2018. Mixed "antiandrogenic" chemicals at low individual doses produce reproductive tract malformations in the male rat. Toxicol. Sci. 164, 166–178.

Cool, J., Defalco, T.J., Capel, B., 2011. Vascular-mesenchymal cross-talk through Vegf and Pdgf drives organ patterning. Proc. Natl. Acad. Sci. U. S. A. 108, 167–172.
Coveney, D., Cool, J., Oliver, T., Capel, B., 2008. Four-dimensional analysis of vascularization during primary development of an organ, the gonad. Proc. Natl. Acad. Sci. U. S. A. 105, 7212–7217.
Culty, M., 2009. Gonocytes, the forgotten cells of the germ cell lineage. Birth Defects Res. C Embryo Today 87, 1–26.
Cunningham, T.J., Duester, G., 2015. Mechanisms of retinoic acid signalling and its roles in organ and limb development. Nat. Rev. Mol. Cell Biol. 16, 110–123.
Daggag, H., Svingen, T., Western, P.S., Bergen, J.A.V.D., McClive, P.J., Harley, V.R., Koopman, P., Sinclair, A.H., 2008. The Rhox homeobox gene family shows sexually dimorphic and dynamic expression during mouse embryonic gonad development1. Biol. Reprod. 79, 468–474.
Defalco, T., Bhattacharya, I., Williams, A.V., Sams, D.M., Capel, B., 2014. Yolk-sac-derived macrophages regulate fetal testis vascularization and morphogenesis. Proc. Natl. Acad. Sci. U. S. A. 111, E2384–E2393.
Dufour, J.M., Vo, M.N., Bhattacharya, N., Okita, J., Okita, R., Kim, K.H., 2003. Peroxisome proliferators disrupt retinoic acid receptor alpha signaling in the testis. Biol. Reprod. 68, 1215–1224.
Edvardsson, U., Bergstrom, M., Alexandersson, M., Bamberg, K., Ljung, B., Dahllof, B., 1999. Rosiglitazone (BRL49653), a PPARgamma-selective agonist, causes peroxisome proliferator-like liver effects in obese mice. J. Lipid Res. 40, 1177–1184.
Ferrara, D., Hallmark, N., Scott, H., Brown, R., McKinnell, C., Mahood, I.K., Sharpe, R.M., 2006. Acute and long-term effects of in utero exposure of rats to di(n-butyl) phthalate on testicular germ cell development and proliferation. Endocrinology 147, 5352–5362.
Fisher, J.S., Macpherson, S., Marchetti, N., Sharpe, R.M., 2003. Human 'testicular dysgenesis syndrome': a possible model using in-utero exposure of the rat to dibutyl phthalate. Hum. Reprod. 18, 1383–1394.
Foster, P.M., 2006. Disruption of reproductive development in male rat offspring following in utero exposure to phthalate esters. Int. J. Androl. 29, 140–147 discussion 181–5.
Franco, H.L., Yao, H.H., 2012. Sex and hedgehog: roles of genes in the hedgehog signaling pathway in mammalian sexual differentiation. Chromosome Res. 20, 247–258.
Furr, J.R., Lambright, C.S., Wilson, V.S., Foster, P.M., Gray Jr., L.E., 2014. A short-term in vivo screen using fetal testosterone production, a key event in the phthalate adverse outcome pathway, to predict disruption of sexual differentiation. Toxicol. Sci. 140, 403–424.
Gaido, K.W., Hensley, J.B., Liu, D., Wallace, D.G., Borghoff, S., Johnson, K.J., Hall, S.J., Boekelheide, K., 2007. Fetal mouse phthalate exposure shows that Gonocyte multinucleation is not associated with decreased testicular testosterone. Toxicol. Sci. 97, 491–503.
Gray, L.E., Lambright, C.S., Conley, J.M., Evans, N., Fur, J.R., Hannas, B.R., Wilson, V.S., Sampson, H., Foster, P.M.D., 2021. Genomic and hormonal biomarkers of phthalate-induced male rat reproductive developmental toxicity part II: A Targeted RT-qPCR array approach that defines a unique adverse outcome pathway. Toxicol. Sci.
Gray, L.E., Furr, J., Lambright, C.S., Evans, N., Hartig, P., Cardon, M., Wilson, V.S., Hotchkiss, A.K., Conley, J., 2020. Quantification of the uncertainties in extrapolating from in vitro androgen receptor (AR) antagonism to in vivo Hershberger Assay endpoints and adverse reproductive development in male rats. Toxicol. Sci.
Gray Jr., L.E., Ostby, J., Furr, J., Price, M., Veeramachaneni, D.N., Parks, L., 2000. Perinatal exposure to the phthalates DEHP, BBP, and DINP, but not DEP, DMP, or DOTP, alters sexual differentiation of the male rat. Toxicol. Sci. 58, 350–365.
Hammond, G.L., 2011. Diverse roles for sex hormone-binding globulin in reproduction1. Biol. Reprod. 85, 431–441.
Hannas, B.R., Furr, J., Lambright, C.S., Wilson, V.S., Foster, P.M., Gray Jr., L.E., 2011a. Dipentyl phthalate dosing during sexual differentiation disrupts fetal testis function and postnatal development of the male Sprague-Dawley rat with greater relative potency than other phthalates. Toxicol. Sci. 120, 184–193.
Hannas, B.R., Lambright, C.S., Furr, J., Howdeshell, K.L., Wilson, V.S., Gray Jr., L.E., 2011b. Dose-response assessment of fetal testosterone production and gene expression levels in rat testes following in utero exposure to diethylhexyl phthalate, diisobutyl phthalate, diisoheptyl phthalate, and diisononyl phthalate. Toxicol. Sci. 123, 206–216.
Hannas, B.R., Lambright, C.S., Furr, J., Evans, N., Foster, P.M., Gray, E.L., Wilson, V.S., 2012. Genomic biomarkers of phthalate-induced male reproductive developmental toxicity: a targeted RT-PCR array approach for defining relative potency. Toxicol. Sci. 125, 544–557.
Heger, N.E., Hall, S.J., Sandrof, M.A., McDonnell, E.V., Hensley, J.B., McDowell, E.N., Martin, K.A., Gaido, K.W., Johnson, K.J., Boekelheide, K., 2012. Human fetal testis xenografts are resistant to phthalate-induced endocrine disruption. Environ. Health Perspect. 120, 1137–1143.
Howdeshell, K.L., Wilson, V.S., Furr, J., Lambright, C.R., Rider, C.V., Blystone, C.R., Hotchkiss, A.K., Gray Jr., L.E., 2008. A mixture of five phthalate esters inhibits fetal testicular testosterone production in the Sprague-Dawley rat in a cumulative, dose-additive manner. Toxicol. Sci. 105, 153–165.
Howdeshell, K.L., Rider, C.V., Wilson, V.S., Furr, J.R., Lambright, C.R., Gray Jr., L.E., 2015. Dose addition models based on biologically relevant reductions in fetal testosterone accurately predict postnatal reproductive tract alterations by a phthalate mixture in rats. Toxicol. Sci. 148, 488–502.
Jobling, M.S., Hutchison, G.R., van den Driesche, S., Sharpe, R.M., 2011. Effects of di(n-butyl) phthalate exposure on foetal rat germ-cell number and differentiation: identification of age-specific windows of vulnerability. Int. J. Androl. 34, e386–e396.
Johnson, K.J., Hensley, J.B., Kelso, M.D., Wallace, D.G., Gaido, K.W., 2007. Mapping gene expression changes in the fetal rat testis following acute dibutyl phthalate exposure defines a complex temporal cascade of responding cell types. Biol. Reprod. 77, 978–989.
Johnson, K.J., McDowell, E.N., Viereck, M.P., Xia, J.Q., 2011. Species-specific dibutyl phthalate fetal testis endocrine disruption correlates with inhibition of SREBP2-dependent gene expression pathways. Toxicol. Sci. 120, 460–474.
Johnson, K.J., Heger, N.E., Boekelheide, K., 2012. Of mice and men (and rats): phthalate-induced fetal testis endocrine disruption is species-dependent. Toxicol. Sci. 129, 235–248.
Jørgensen, A., Macdonald, J., Nielsen, J.E., Kilcoyne, K.R., Perlman, S., Lundvall, L., Langhoff thuesen, L., Juul Hare, K., Frederiksen, H., Andersson, A.M., Skakkebæk, N. E., Juul, A., Sharpe, R.M., Rajpert-De Meyts, E., Mitchell, R.T., 2018. Nodal signaling regulates germ cell development and establishment of seminiferous cords in the human fetal testis. Cell Rep 25, 1924–1937.e4.
Kapoor, D., Channer, K.S., Jones, T.H., 2008. Rosiglitazone increases bioactive testosterone and reduces waist circumference in hypogonadal men with type 2 diabetes. Diab. Vasc. Dis. Res. 5, 135–137.
Kashimada, K., Svingen, T., Feng, C.W., Pelosi, E., Bagheri-Fam, S., Harley, V.R., Schlessinger, D., Bowles, J., Koopman, P., 2011. Antagonistic regulation of Cyp26b1 by transcription factors SOX9/SF1 and FOXL2 during gonadal development in mice. FASEB J. 25, 3561–3569.
Kavlock, R., Boekelheide, K., Chapin, R., Cunningham, M., Faustman, E., Foster, P., Golub, M., Henderson, R., Hinberg, I., Little, R., Seed, J., Shea, K., Tabacova, S., Tyl, R., Williams, P., Zacharewski, T., 2002. NTP Center for the Evaluation of Risks to Human Reproduction: phthalates expert panel report on the reproductive and developmental toxicity of di-n-hexyl phthalate. Reprod. Toxicol. 16 (5), 709–719.
Kavlock, R., Barr, D., Boekelheide, K., Breslin, W., Breysse, P., Chapin, R., Gaido, K., Hodgson, E., Marcus, M., Shea, K., Williams, P., 2006. NTP-CERHR expert panel update on the reproductive and developmental toxicity of di(2-ethylhexyl) phthalate. Reprod. Toxicol. 22, 291–399.
Kleymenova, E., Swanson, C., Boekelheide, K., Gaido, K.W., 2005. Exposure in utero to di (n-butyl) phthalate alters the vimentin cytoskeleton of fetal rat Sertoli cells and disrupts Sertoli cell-gonocyte contact. Biol. Reprod. 73, 482–490.
Koubova, J., Menke, D.B., Zhou, Q., Capel, B., Griswold, M.D., Page, D.C., 2006. Retinoic acid regulates sex-specific timing of meiotic initiation in mice. Proc. Natl. Acad. Sci. U. S. A. 103, 2474–2479.
Koubova, J., Hu, Y.C., Bhattacharyya, T., Soh, Y.Q., Gill, M.E., Goodheart, M.L., Hogarth, C.A., Griswold, M.D., Page, D.C., 2014. Retinoic acid activates two pathways required for meiosis in mice. PLoS Genet. 10, e1004541.
Lambrot, R., Coffigny, H., Pairault, C., Donnadieu, A.C., Frydman, R., Habert, R., Rouiller-Fabre, V., 2006. Use of organ culture to study the human fetal testis development: effect of retinoic acid. J. Clin. Endocrinol. Metab. 91, 2696–2703.
Lambrot, R., Muczynski, V., Lecureuil, C., Angenard, G., Coffigny, H., Pairault, C., Moison, D., Frydman, R., Habert, R., Rouiller-Fabre, V., 2009. Phthalates impair germ cell development in the human fetal testis in vitro without change in testosterone production. Environ. Health Perspect. 117, 32–37.
Laurent, M.R., Hammond, G.L., Blokland, M., Jardí, F., Antonio, L., Dubois, V., Khalil, R., Sterk, S.S., Gielen, E., Decallonne, B., Carmeliet, G., Kaufman, J.M., Fiers, T., Huhtaniemi, I.T., Vanderschueren, D., Claessens, F., 2016a. Sex hormone-binding globulin regulation of androgen bioactivity in vivo: validation of the free hormone hypothesis. Sci. Rep. 6, 35539.
Laurent, M.R., Helsen, C., Antonio, L., Schollaert, D., Joniau, S., Vos, M.J., Decallonne, B., Hammond, G.L., Vanderschueren, D., Claessens, F., 2016b. Effects of sex hormone-binding globulin (SHBG) on androgen bioactivity in vitro. Mol. Cell. Endocrinol. 437, 280–291.
Lee, Florence Y., Faivre, Emily J., Suzawa, M., Lontok, E., Ebert, D., Cai, F., Belsham, Denise D., Ingraham, Holly A., 2011. Eliminating SF-1 (NR5A1) sumoylation in vivo results in ectopic hedgehog signaling and disruption of endocrine development. Dev. Cell 21, 315–327.
Lehraiki, A., Racine, C., Krust, A., Habert, R., Levacher, C., 2009. Phthalates impair germ cell number in the mouse fetal testis by an androgen- and estrogen-independent mechanism. Toxicol. Sci. 111, 372–382.
Lei, N., Heckert, L.L., 2002. Sp1 and Egr1 regulate transcription of the Dmrt1 gene in Sertoli cells. Biol. Reprod. 66, 675–684.
Leng, Y., Sun, Y., Huang, W., Lv, C., Cui, J., Li, T., Wang, Y., 2020. Phthalate esters and dexamethasone synergistically activate glucocorticoid receptor. J. Environ. Sci. Health, Part A 1–8.
Li, H., Spade, D.J., 2021. Reproductive toxicology: environmental exposures, fetal testis development and function: phthalates and beyond. Reproduction 162, F147–F167.
Livera, G., Rouiller-Fabre, V., Durand, P., Habert, R., 2000. Multiple effects of retinoids on the development of Sertoli, germ, and Leydig cells of fetal and neonatal rat testis in culture. Biol. Reprod. 62, 1303–1314.
Maclean, G., Li, H., Metzger, D., Chambon, P., Petkovich, M., 2007. Apoptotic extinction of germ cells in testes of Cyp26b1 knockout mice. Endocrinology 148, 4560–4567.
Main, K.M., Mortensen, G.K., Kaleva, M.M., Boisen, K.A., Damgaard, I.N., Chellakooty, M., Schmidt, I.M., Suomi, A.M., Virtanen, H.E., Petersen, D.V., Andersson, A.M., Toppari, J., Skakkebaek, N.E., 2006. Human breast milk contamination with phthalates and alterations of endogenous reproductive hormones in infants three months of age. Environ. Health Perspect. 114, 270–276.
Manikkam, M., Guerrero-Bosagna, C., Tracey, R., Haque, M.M., Skinner, M.K., 2012. Transgenerational actions of environmental compounds on reproductive disease and identification of epigenetic biomarkers of ancestral exposures. PLoS ONE 7, e31901.
Manikkam, M., Tracey, R., Guerrero-Bosagna, C., Skinner, M.K., 2013. Plastics derived endocrine disruptors (BPA, DEHP and DBP) induce epigenetic transgenerational

inheritance of obesity, reproductive disease and sperm epimutations. PLoS ONE 8, e55387.
Mazaud-Guittot, S., Meugnier, E., Pesenti, S., Wu, X., Vidal, H., Gow, A., Le Magueresse-Battistoni, B., 2010. Claudin 11 deficiency in mice results in loss of the sertoli cell epithelial phenotype in the testis1. Biol. Reprod. 82, 202–213.
Mazaud-Guittot, S., Gow, A., Le Magueresse-Battistoni, B., 2011. Phenotyping the claudin 11 deficiency in testis: from histology to immunohistochemistry. Methods Mol. Biol. 763, 223–236.
Mitchell, R.T., Childs, A.J., Anderson, R.A., van den Driesche, S., Saunders, P.T., McKinnell, C., Wallace, W.H., Kelnar, C.J., Sharpe, R.M., 2012. Do phthalates affect steroidogenesis by the human fetal testis? Exposure of human fetal testis xenografts to di-n-butyl phthalate. J. Clin. Endocrinol. Metab. 97, E341–E348.
Mitola, S., Ravelli, C., Moroni, E., Salvi, V., Leali, D., Ballmer-Hofer, K., Zammataro, L., Presta, M., 2010. Gremlin is a novel agonist of the major proangiogenic receptor VEGFR2. Blood 116, 3677–3680.
Muczynski, V., Cravedi, J.P., Lehraiki, A., Levacher, C., Moison, D., Lecureuil, C., Messiaen, S., Perdu, E., Frydman, R., Habert, R., Rouiller-Fabre, V., 2012. Effect of mono-(2-ethylhexyl) phthalate on human and mouse fetal testis: In vitro and in vivo approaches. Toxicol. Appl. Pharmacol. 261, 97–104.
Mylchreest, E., Sar, M., Wallace, D.G., Foster, P.M., 2002. Fetal testosterone insufficiency and abnormal proliferation of Leydig cells and gonocytes in rats exposed to di(n-butyl) phthalate. Reprod. Toxicol. 16, 19–28.
Nef, S., Parada, L.F., 1999. Cryptorchidism in mice mutant for Insl3. Nat. Genet. 22, 295–299.
Nicol, B., Grimm, S.A., Gruzdev, A., Scott, G., Ray, M.K., Yao, H.H., 2018. Genome-wide identification of FOXL2 binding and characterization of FOXL2 feminizing action in the fetal gonads. Hum. Mol. Genet.
Nicol, B., Grimm, S.A., Chalmel, F., Lecluze, E., Pannetier, M., Pailhoux, E., Dupin-De-beyssat, E., Guiguen, Y., Capel, B., Yao, H.H.C., 2019. RUNX1 maintains the identity of the fetal ovary through an interplay with FOXL2. Nat. Commun. 10, 5116.
Nicol, B., Yao, H.H., 2015. Gonadal identity in the absence of pro-testis factor SOX9 and pro-ovary factor beta-catenin in mice. Biol. Reprod. 93, 35.
Ottolenghi, C., Pelosi, E., Tran, J., Colombino, M., Douglass, E., Nedorezov, T., Cao, A., Forabosco, A., Schlessinger, D., 2007. Loss of Wnt4 and Foxl2 leads to female-to-male sex reversal extending to germ cells. Hum. Mol. Genet. 16, 2795–2804.
Parks, L.G., Ostby, J.S., Lambright, C.R., Abbott, B.D., Klinefelter, G.R., Barlow, N.J., Gray Jr., L.E., 2000. The plasticizer diethylhexyl phthalate induces malformations by decreasing fetal testosterone synthesis during sexual differentiation in the male rat. Toxicol. Sci. 58, 339–349.
Raymond, C.S., Murphy, M.W., O'Sullivan, M.G., Bardwell, V.J., Zarkower, D., 2000. Dmrt1, a gene related to worm and fly sexual regulators, is required for mammalian testis differentiation. Genes Dev. 14, 2587–2595.
Sarath Josh, M.K., Pradeep, S., Vijayalekshmi Amma, K.S., Balachandran, S., Abdul Jaleel, U.C., Doble, M., Spener, F., Benjamin, S., 2014. Phthalates efficiently bind to human peroxisome proliferator activated receptor and retinoid X receptor alpha, beta, gamma subtypes: an in silico approach. J. Appl. Toxicol. 34, 754–765.
Spade, D.J., Hall, S.J., Saffarini, C.M., Huse, S.M., McDonnell, E.V., Boekelheide, K., 2014. Differential response to abiraterone acetate and di-n-butyl phthalate in an androgen-sensitive human fetal testis xenograft bioassay. Toxicol. Sci. 138, 148–160.
Spade, D.J., Hall, S.J., Wilson, S., Boekelheide, K., 2015. Di-n-butyl phthalate induces multinucleated germ cells in the rat fetal testis through a nonproliferative mechanism. Biol. Reprod. 93, 110.
Spade, D.J., Bai, C.Y., Lambright, C., Conley, J.M., Boekelheide, K., Gray, L.E., 2018. Validation of an automated counting procedure for phthalate-induced testicular multinucleated germ cells. Toxicol. Lett. 290, 55–61.
Spade, D.J., Dere, E., Hall, S.J., Schorl, C., Freiman, R.N., Boekelheide, K., 2019a. All-trans retinoic acid disrupts development in ex vivo cultured fetal rat testes. I: Altered seminiferous cord maturation and testicular cell fate. Toxicol. Sci. 167, 546–558.
Spade, D.J., Hall, S.J., Wortzel, J.D., Reyes, G., Boekelheide, K., 2019b. All-trans retinoic acid disrupts development in ex vivo cultured fetal rat testes. II: Modulation of mono-(2-ethylhexyl) phthalate toxicity. Toxicol. Sci. 168, 149–159.
Tian, R.H., Yang, S., Zhu, Z.J., Wang, J.L., Liu, Y., Yao, C., Ma, M., Guo, Y., Yuan, Q., Hai, Y., Huang, Y.R., He, Z., Li, Z., 2015. NODAL secreted by male germ cells regulates the proliferation and function of human Sertoli cells from obstructive azoospermia and nonobstructive azoospermia patients. Asian J Androl 17, 996–1005.
Torres, M., Gómez-Pardo, E., Dressler, G.R., Gruss, P., 1995. Pax-2 controls multiple steps of urogenital development. Development 121, 4057–4065.
Tourtellotte, W.G., Nagarajan, R., Auyeung, A., Mueller, C., Milbrandt, J., 1999. Infertility associated with incomplete spermatogenic arrest and oligozoospermia in Egr4-deficient mice. Development 126, 5061–5071.
Trautmann, E., Guerquin, M.J., Duquenne, C., Lahaye, J.B., Habert, R., Livera, G., 2008. Retinoic acid prevents germ cell mitotic arrest in mouse fetal testes. Cell Cycle 7, 656–664.
van den Driesche, S., Kolovos, P., Platts, S., Drake, A.J., Sharpe, R.M., 2012. Inter-relationship between testicular dysgenesis and Leydig cell function in the masculinization programming window in the rat. PLoS ONE 7, e30111.
Veeramachaneni, D.N., Klinefelter, G.R., 2014. Phthalate-induced pathology in the foetal testis involves more than decreased testosterone production. Reproduction 147, 435–442.
Wang, Y., Yang, Q., Liu, W., Yu, M., Zhang, Z., Cui, X., 2016. Di(2-ethylhexyl) phthalate exposure in utero damages sertoli cell differentiation via disturbance of sex determination pathway in fetal and postnatal mice. Toxicol. Sci. 152, 53–61.
Weiss, J., Meeks, J.J., Hurley, L., Raverot, G., Frassetto, A., Jameson, J.L., 2003. Sox3 is required for gonadal function, but not sex determination, in males and females. Mol. Cell. Biol. 23, 8084–8091.
Welborn, J.P., Davis, M.G., Ebers, S.D., Stodden, G.R., Hayashi, K., Cheatwood, J.L., Rao, M.K., Maclean 2nd, J.A., 2015. Rhox8 Ablation in the sertoli cells using a tissue-specific RNAi approach results in impaired male fertility in mice. Biol. Reprod. 93, 8.
Wu, Q., Kanata, K., Saba, R., Deng, C.-X., Hamada, H., Saga, Y., 2013. Nodal/activin signaling promotes male germ cell fate and suppresses female programming in somatic cells. Development 140, 291–300.
Zhang, J., Hu, G., Huang, B., Zhuo, D., Xu, Y., Li, H., Zhan, X., Ge, R.-S., Xu, Y., 2019. Dexamethasone suppresses the differentiation of stem Leydig cells in rats in vitro. BMC Pharmacol. Toxicol. 20, 32.
Zhao, J., Lu, P., Wan, C., Huang, Y., Cui, M., Yang, X., Hu, Y., Zheng, Y., Dong, J., Wang, M., Zhang, S., Liu, Z., Bian, S., Wang, X., Wang, R., Ren, S., Wang, D., Yao, Z., Chang, G., Tang, F., Zhao, X.-Y., 2021. Cell-fate transition and determination analysis of mouse male germ cells throughout development. Nat. Commun. 12, 6839.